Journal of Medicinal Chemistry

Article

Second generation of Mannich base type derivatives with in vivo activity against Trypanosoma cruzi

Rubén Martín-Escolano, Elsa Moreno-Viguri, Mery Jhenny Santiváñez Veliz, Álvaro Martín-Montes, Encarnación Medina-Carmona, Rocío Paucar, Clotilde Marín, Amaya Azqueta, Nuria Cirauqui, Angel Luis Pey, Silvia Pérez-Silanes, and Manuel Sánchez-Moreno

J. Med. Chem., **Just Accepted Manuscript** • DOI: 10.1021/acs.jmedchem.8b00468 • Publication Date (Web): 08 Jun 2018

Just Accepted

ACS Publications

is published by the American Chemical Society. 1155 Sixteenth Street N.W., Washington, DC 20036

Second generation of Mannich base type derivatives with *in vivo* activity against *Trypanosoma cruzi*.

Rubén Martín-Escolano[1], Elsa Moreno-Viguri[2], Mery Santivañez-Veliz[2], Alvaro Martin-Montes[1], Encarnación Medina-Carmona[3], Rocío Paucar[2], Clotilde Marín[1]*, Amaya Azqueta[4], Nuria Cirauqui[5], Angel L. Pey[3], Silvia Pérez-Silanes[2]* and Manuel Sánchez-Moreno[1]*.

[1]Departament of Parasitology, Instituto de Investigación Biosanitaria (ibs.Granada), Hospitales Universitarios De Granada/University of Granada, Severo Ochoa s/n, E-18071 Granada, Spain.

[2]Universidad de Navarra, Department of Organic and Pharmaceutical Chemistry, Instituto de Salud Tropical, Pamplona 31008, Spain.

[3]Department of Physical Chemistry, Faculty of Sciences, University of Granada, Av. Fuentenueva s/n, 18071, Granada, Spain.

[4] Universidad de Navarra, Department of Pharmacology and Toxicology, Pamplona 31008, Spain.

[5]Department of Pharmaceutical Sciences, Federal University of Rio de Janeiro, Rio de Janeiro 21949-900, Brazil.

ABSTRACT

Chagas Disease is a potentially life-threatening and neglected tropical disease caused by *Trypanosoma cruzi*. One of the most important challenges related to Chagas disease is the search for new, safe, effective and affordable drugs since the current therapeutic arsenal is inadequate and insufficient. Here, we report a simple and cost-effective synthesis and the biological evaluation of the second generation of Mannich base-type derivatives. Compounds **7**, **9** and **10** showed improved *in vitro* efficiency and lower toxicity than benznidazole, in addition to no genotoxicity; thus, they were applied in *in vivo* assays to assess their activity in both acute and chronic phases of the

disease. Compound **10** presented a similar profile to benznidazole from the parasitological perspective but also yielded encouraging data, as no toxicity was observed. Moreover, compound **9** showed lower parasitaemia and higher curative rates than benznidazole, also with lower toxicity in both acute and chronic phases. Therefore, further studies should be considered to optimize compound **9** to promote its further preclinical evaluation.

KEYWORDS: arylaminoketone, Mannich Bases, Superoxide dismutase, *Trypanosoma cruzi*, Chagas disease.

INTRODUCTION

Chagas disease (CD) is a chronic parasitosis caused by the protozoan parasite *Trypanosoma cruzi* (*T. cruzi*). CD is endemic in 21 American countries [1-3]; however, the disease has become a public health concern in non-endemic countries, such as the United States, Canada and some European countries, due to the appearance of non-vector transmission through blood transfusions and organ transplants and congenital transmission associated with massive migratory movements [4, 5]. According to World Health Organization (WHO) data, CD affects approximately 5.7 million people to cause approximately 7,000 deaths annually, and almost 70 million people are at risk of infection [6, 7]. The disease also causes approximately 0.6 million disability-adjusted life years with further economic depression of the affected areas.

Progress in the control of infection transmission routes has not been accompanied by progress in the development of new treatments for the disease due to different factors, such as a lack of knowledge about the pathophysiology of the disease, the high level of biological and genetic polymorphism presented by the parasite depending on the geographical region and the lack of pharmaceutical company interest. In addition, the experimental tools available for *in vitro* and *in vivo* testing have had a low predictive value [8-12].

For these reasons, there is no effective chemotherapy; indeed, only two drugs developed in the 60s, nifurtimox (NFX, Lampit®, Bayer) and benznidazole (BZN, Rochagan®, Radanil®, Roche), are currently available. Both drugs present important limitations, such as low efficacy during the chronic phase of the disease, different activities against various genetic lineages of *T. cruzi*, numerous side effects in patients and a complicated treatment dosage. Based on its relatively better toxicity profile and accumulated experience, BZN is considered the current standard of treatment; however, it remains inefficient in the chronic phase of the disease and has unacceptable toxicity [13, 14]. Moreover, no drugs have been authorized for the treatment of adults, and only a paediatric formulation of BZN has recently been approved by the Food and Drug Administration (FDA) [15].

Furthermore, the most promising nitroimidazoles, such as posaconazole and ravuconazole, have not shown the expected good results in clinical trials, and their development has been discontinued [16-18].

In recent years, important advances have been achieved in the field of molecular biology and genomics of *T. cruzi* and in CD pathophysiology. As a result, more research groups and pharmaceutical companies are investing the development of new drugs. However, no success has been achieved in developing a drug for CD that fulfils the target product profile (TPP) proposed by the DND*i* [19, 20].

In a previous study, our group identified new Mannich base-type derivatives that showed high *in vitro* activity against different life cycle stages and parasite strains of *T. cruzi* [21]. The lead compounds showed high selectivity indexes (SIs), curative activity during the acute phase of the disease and prevention of parasitaemia reactivation after immunosuppressive treatment, demonstrating curative rates by polymerase chain reaction (PCR) higher than BZN in a murine *in vivo* model. In addition, the compounds were not mutagenic or genotoxic [21].

Here we present the synthesis, *in vitro* anti-*T. cruzi* activity and cytotoxicity of a second generation of arylaminoketone Mannich base derivatives designed following our previous study, with the aim of identifying a cost-effective route that may allow the broad study of substituents. IC_{50} values lower than 10 μM, SI higher than 50 and an absence of genotoxicity in the SOS/umu screening test have been established as the cut-off to further evaluate compounds for *in vivo* activity, in both acute and chronic phases of the disease. Moreover, the possible mechanisms of action of the new compounds have been studied in terms of the variations in excreted metabolite patterns, alterations of mitochondrial membrane potential and Fe-Superoxide dismutase (Fe-SOD) inhibition. Taken together, these new series led us to an interesting new lead for the development of anti-Chagas treatment, which demonstrated both a good activity/selectivity profile and a cost-effective synthetic route.

COMPOUND DESIGN

Mannich bases are considered important pharmacophores with high potential in the field of medical chemistry and have shown a wide spectrum of biological activities [20, 22] as anti-inflammatory [23], anticancer [24-25], antibacterial [26], antifungal [27], antituberculosis [28] and antimalarial activities [29]. In addition, Mannich bases endowed with biological activity against *T. brucei* multiresistant strains [30] as well as with inhibitory activity against *T. cruzi* trypanothione reductase (TRase) have also been described [31].

The simplicity and cost-effectiveness of the synthetic methodologies used in the drug discovery process against neglected tropical diseases (NTD) play a key role. Taking advantage of the Mannich reaction as a powerful tool for C-C bonding in organic reaction and considering the great potential of Mannich base scaffolds as antiparasitic agents, we designed a second generation of *β*-aminoketones by modification of the previously identified lead compounds [21] (**Figure 1**).

Our previous docking results on the Fe-SOD enzyme (compounds **A** and **B** in **Figure 1A**) showed that the carbonyl group (in red in **Figure 1B**), cyclic amine (in blue in **Figure 1B**) and the following phenyl group (in green in **Figure 1B**) bind similarly in all compounds, with the phenyl ring performing π-stacking interactions with Phe123 and the cyclic amine bound close to Glu166. Therefore, we believe that these groups are the most important for binding to the SOD enzyme; thus, they were retained in the new series we present herein. In contrast, the benzothiophene ring was substituted with a mono or di-substituted benzene ring (in purple in **Figure 1B**), which allows easier and lower-cost coverage of modifications by including different electronic character substituents. For the some reason we included only piperazine ring as cyclic amine. Fluorine atoms have been substituted in different positions of the phenyl rings because fluorine is a well-known hydrogen mimic. This strategy is one of the most classical bioisosteric replacements used in medicinal chemistry. The trifluoromethyl moiety was also included with the same purpose of enhancing metabolic stability. Nevertheless, some other halogens, methyl and methoxy moieties were also included to explore their influence on the efficacy, toxicity and pharmacokinetic

(PK)/pharmacodinamic (PD) properties so that a structure-activity relationship could be explored. We decided to retain the piperazine scaffold as constant in the general chemical skeleton considering that the incorporation of cyclic amines is widely used in the search for biologically active molecules, and previous studies by our group have confirmed interest in this amine. Several examples of anti-trypanosomatid agents based on cyclic amines have been reported [21, 32-35], and antifungal drugs with anti-kinetoplastid activity, such as ketoconazole, itraconazole or posaconazole, present piperazine rings in their structures [36-39]. Moreover, we examined an increasing length of the linker between the piperazine and the phenyl group, which may allow improved binding of piperazine to the negative chain of Glu166 (in magenta in **Figure 1B**). Considering that the predicted pKa of our compounds suggests equilibrium between a neutral and a positively charged piperazine (at the nitrogen closer to the carbonyl group, in bold in **Figure 1B**), we believe that its interaction with the negative side chain of Glu166 must be important for affinity. This design also took into consideration the increment of chemical variability of β-aminoketones, cost-efficient chemistry and synthetic simplicity, which are essential factors for attracting the attention and interest of pharmaceutical companies.

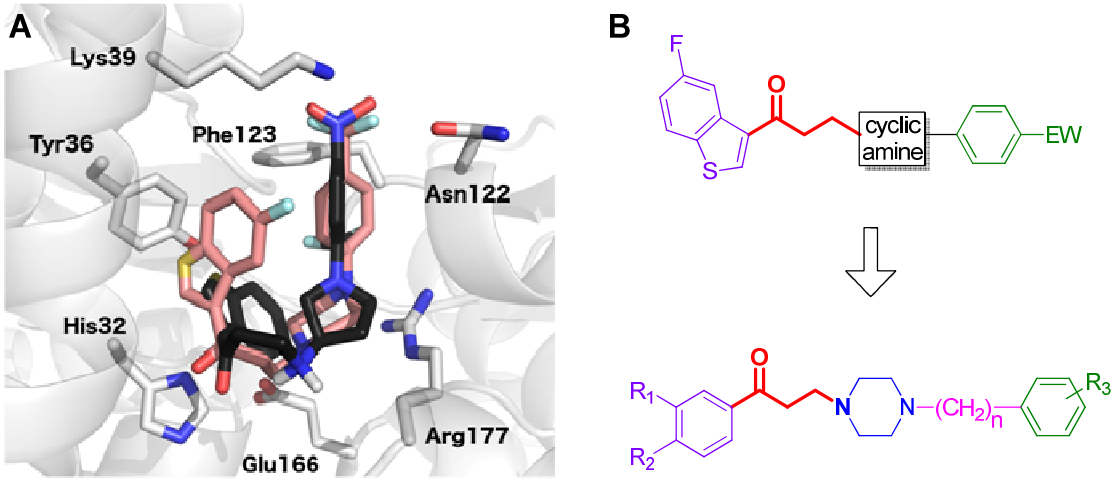

Figure 1. A) Docking results of our previous leads (in pale pink and black compounds 4 and 10 respectively from Moreno-Viguri et al., 2016) on the Fe-SOD enzyme, showing the conserved binding mode for the carbonyl, cyclic amine and phenyl scaffolds, while the benzothiophene ring

presents different positioning in each compound. B) Design of the new series of arylaminoketone Mannich Base type derivatives. Simplified scheme of the new series design (down) based on our previous leads (up). The different groups are colored as mentioned on the text.

RESULTS AND DISCUSSION

Chemistry.

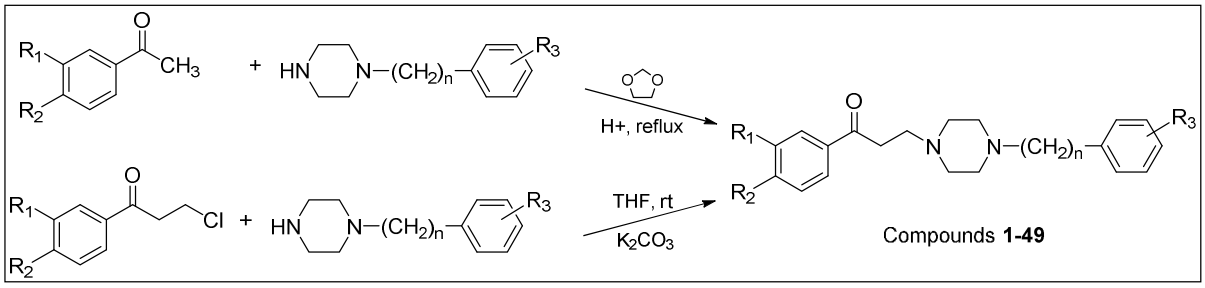

Figure 2. Synthesis of new arylaminoketone derivatives.

Forty-four out of forty-nine compounds (**2-17**, **22-49**) were obtained by Mannich reaction as previously reported [21]. Compounds **18-21** were obtained by an aliphatic nucleophilic substitution in which the corresponding piperazine was condensed with a primary alkyl halide in the presence of K_2CO_3 as base and tetrahydrofuran (THF) as solvent (**Figure 2)**. The synthetic methodology to obtain compound **1** has been previously described [40]. Therefore, 48 new derivatives have been synthesized using a simple, fast and economically affordable methodology.

Table 1. Structure and molecular properties of the new compounds calculated with the DataWarrior program [41].

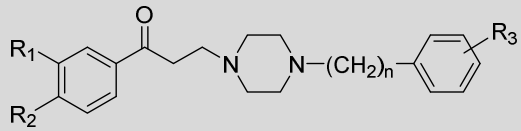					Molecular properties					
Comp	**R_1**	**R_2**	**n**	**R_3**	**MW[b]**	**clogP[c]**	**clogS[d]**	**PSA[e]**	**HBA[f]**	**HBD[g]**
1[a]	H	H	0	4-F	313.4	0.8	-3.4	24.7	3	1
2	H	H	0	4-CF_3	363.4	1.6	-3.9	24.7	3	1
3	H	CH_3	0	4-F	327.4	1.2	-3.8	24.7	3	1
4	H	CH_3	0	4-CF_3	377.4	1.9	-4.2	24.7	3	1

5	H	CH_3	0	4-Cl	343.9	1.7	-4.2	24.7	3	1
6	H	CH_3	0	4-NO_2	354.4	1.5	-3.9	70.5	6	1
7	H	OCH_3	0	4-F	343.4	0.7	-3.4	34.0	4	1
8	H	OCH_3	0	4-CF_3	393.4	1.5	-3.9	34.0	4	1
9	H	OCH_3	0	4-Cl	359.9	1.3	-3.9	34.0	4	1
10	H	OCH_3	0	4-NO_2	370.4	1.1	-3.6	79.8	7	1
11	OCH_3	OCH_3	0	4-F	373.4	0.7	-3.4	43.2	5	1
12	OCH_3	OCH_3	0	4-CF_3	423.4	1.4	-3.9	43.2	5	1
13	OCH_3	OCH_3	0	4-Cl	389.9	1.2	-3.9	43.2	5	1
14	OCH_3	OCH_3	0	4-NO_2	400.4	1.0	-3.6	89.0	8	1
15	OCH_3	OCH_3	1	3-F	373.4	0.7	-3.5	43.2	5	1
16	OCH_3	OCH_3	1	H	355.5	0.6	-3.1	43.2	5	1
17	OCH_3	OCH_3	1	3-CH_3	369.5	0.9	-3.5	43.2	5	1
18	H	F	0	2-OCH_3	327.4	1.2	-3.8	24.7	3	1
19	H	F	0	2-F	331.4	0.9	-3.7	24.7	3	1
20	H	F	0	4-OCH_3	343.4	0.8	-3.4	34.0	4	1
21	H	F	0	4-NO_2	358.4	1.2	-3.9	70.6	6	1
22	H	Br	0	4-F	392.3	1.6	-4.2	24.7	3	1
23	H	Br	0	4-CF_3	442.3	2.3	-4.7	24.7	3	1
24	H	Br	0	4-Cl	408.7	2.1	-4.7	24.7	3	1
25	H	Br	0	4-NO_2	419.3	1.9	-4.4	70.6	6	1
26	Br	F	0	4-F	410.3	1.7	-4.6	24.7	3	1
27	Br	F	0	4-CF_3	460.3	2.4	-5.0	24.7	3	1
28	Br	F	0	4-Cl	426.7	2.2	-5.0	24.7	3	1
29	Br	F	0	4-NO_2	437.3	2.0	-4.7	70.6	6	1
30	F	F	0	4-F	349.3	1.0	-4.0	24.7	3	1
31	F	F	0	4-CF_3	399.4	1.8	-4.5	24.7	3	1

32	F	F	0	4-Cl	365.8	1.5	-4.5	24.7	3	1
33	F	F	0	4-NO_2	376.4	1.3	-4.2	70.6	6	1
34	Cl	F	0	4-F	365.8	1.5	-4.5	24.7	3	1
35	Cl	F	0	4-CF_3	415.8	2.3	-4.9	24.7	3	1
36	Cl	F	0	4-Cl	382.3	2.1	-4.9	24.7	3	1
37	Cl	F	0	4-NO_2	392.8	1.8	-4.6	70.6	6	1
38	F	Cl	0	4-F	365.8	1.5	-4.5	24.7	3	1
39	F	Cl	0	4-CF_3	415.8	2.3	-4.9	24.7	3	1
40	F	Cl	0	4-Cl	382.3	2.1	-4.9	24.7	3	1
41	F	Cl	0	4-NO_2	392.8	1.8	-4.6	70.6	6	1
42	H	CF_3	0	4-F	381.4	1.7	-4.2	24.7	3	1
43	H	CF_3	0	4-CF_3	413.4	2.3	-4.6	24.7	3	1
44	H	CF_3	0	4-Cl	397.8	2.2	-4.6	24.7	3	1
45	H	CF_3	0	4-NO_2	408.4	2.0	-4.3	70.6	6	1
46	H	OCF_3	0	4-F	397.4	1.9	-4.4	34.0	4	1
47	H	OCF_3	0	4-CF_3	447.4	2.7	-4.9	34.0	4	1
48	H	OCF_3	0	4-Cl	413.9	2.4	-4.9	34.0	4	1
49	H	OCF_3	0	4-NO_2	424.4	2.2	-4.6	79.8	7	1

a: Previously published. [b]Total Molecular Weight ($g \cdot mol^{-1}$). [c]Logarithm of the partition coefficient between n-octanol and water. [d]Logarithm of the solubility measured in $mol \cdot L^{-1}$. [e]Polar Surface Area ($Å^2$). [f]Number of hydrogen-bond acceptors. [g]Number of hydrogen-bond donors.

The results of the *in silico* study of some relevant molecular properties related to the drug-likeness of the compounds are shown in **Table 1**. It can be observed that all compounds fulfil the Lipinski "rule of five", with a molecular weight lower than 500 $g \cdot mol^{-1}$, an estimated partition coefficient (logP) lower than 5, a number of hydrogen-bond acceptors lower than 10, and less than 5 hydrogen bond donors. Moreover, the polar surface area (PSA) and aqueous solubility (logS) values

anticipate good oral bioavailability, with the first being lower than 140 $Å^2$ and the second similar or higher than -4.

***In vitro* trypanocidal evaluation.**

The genetic diversity of *T. cruzi* is extensively acknowledged. Currently, *T. cruzi* is divided into seven discrete typing units (DTUs), presenting different genotypes and phenotypes, ecological and epidemiological associations, evolutionary relationships, pathogenesis, tropism and drug resistance [42]. Consequently, three different *T. cruzi* strains (TcI, TcV and TcVI), with different tropisms, hosts and locations, were used to determine and select those compounds with good performance.

The extracellular epimastigote-like form is habitually used because of its simple culture and maintenance in the laboratory. However, tests against the developed forms in vertebrate hosts, bloodstream trypomastigotes and intracellular amastigote forms (responsible for the chronic phase of CD), are more appropriate [43]. For this reason, the *in vitro* trypanocidal activity of compounds **1-49** and the reference drug BZN were evaluated in the epimastigote form with the objective of establishing the inhibition concentrations 50 (IC_{50} values) as a primary screen.

Table 2 shows the IC_{50} values of the compounds on the epimastigote forms of the three *T. cruzi* strains cited above, the cytotoxicity using mammalian Vero cells and the selectivity index (SI = IC_{50} Vero cells/IC_{50} epimastigote forms). Interestingly, almost all these Mannich base-type derivatives were substantially less toxic than the reference drug BZN after 72 h of exposure at different concentrations.

Table 2. *In vitro* activity, cytotoxicity and selectivity index for compounds on the epimastigote form of *Trypanosoma cruzi* strains.

Comp	Activity IC_{50} (µM)[a]			Toxicity IC_{50} Vero Cell (µM)[b]	Selectivity Index[c]		
	T. cruzi Arequipa strain	*T. cruzi* SN3 strain	*T. cruzi* Tulahuen strain		*T. cruzi* Arequipa strain	*T. cruzi* SN3 strain	*T. cruzi* Tulahuen strain
BZN	16.9 ± 1.8	36.2 ± 2.4	19.7 ± 1.7	23.2 ± 2.1	1.4	0.6	1.2

1	65.7 ± 5.7	32.9 ± 2.9	94.1 ± 7.9	13.4 ± 1.4	0.2 (0)	0.4 (1)	0.1 (0)
2	12.8 ± 1.3	16.2 ± 1.5	24.9 ± 3.1	15.7 ± 1.7	1.2 (1)	1.0 (2)	0.6 (1)
3	43.5 ± 4.8	78.8 ± 6.7	25.0 ± 2.1	55.4 ± 4.2	1.3 (1)	0.7 (1)	2.2 (2)
4	14.2 ± 1.7	17.6 ± 1.5	22.5 ± 2.3	139.7 ± 12.4	9.8 (7)	7.9 (12)	6.2 (5)
5	31.7 ± 2.9	26.0 ± 2.4	29.5 ± 3.1	183.8 ± 157	5.8 (4)	7.1 (11)	6.2 (5)
6	28.4 ± 3.1	18.2 ± 1.4	46.2 ± 4.5	234.6 ± 17.8	8.3 (6)	12.9 (20)	5.1 (4)
7	1.4 ± 0.1	2.0 ± 0.1	1.8 ± 0.2	55.0 ± 4.9	40.2 (29)	27.9 (44)	30.2 (26)
8	72.9 ± 6.7	32.3 ± 3.5	44.0 ± 4.9	135.2 ± 11.0	1.9 (1)	4.2 (7)	3.1 (3)
9	9.5 ± 0.8	6.3 ± 0.5	7.3 ± 0.6	300.0 ± 24.1	31.5 (23)	47.8 (75)	40.9 (35)
10	31.6 ± 0.3	22.0 ± 0.2	37.4 ± 0.4	587.2 ± 37.6	18.6 (14)	26.7 (4)	15.7 (13)
11	153.8 ± 14.2	61.5 ± 6.7	103.3 ± 9.4	174.8 ± 16.8	1.1 (1)	2.8 (4)	1.7 (1)
12	59.0 ± 6.2	27.8 ± 3.2	33.9 ± 3.1	242.5 ± 21.0	4.1 (3)	8.7 (14)	7.2 (6)
13	90.3 ± 8.9	43.9 ± 4.5	36.6 ± 3.8	185.4 ± 14.8	2.1 (1)	4.2 (7)	5.1 (4)
14	94.5 ± 9.7	173.6 ± 19.8	104.9 ± 11.2	105.2 ± 8.9	1.1 (1)	0.6 (1)	1.0 (1)
15	49.0 ± 5.1	48.0 ± 5.0	40.8 ± 4.5	22.4 ± 3.8	0.5 (0)	0.5 (1)	0.6 (0)
16	29.5 ± 3.0	55.2 ± 6.1	46.2 ± 4.1	47.5 ± 5.7	1.6 (1)	0.9 (1)	1.0 (1)
17	19.4 ± 2.1	24.1 ± 2.4	28.4 ± 2.4	52.0 ± 4.9	2.7 (2)	2.2 (3)	1.8 (2)
18	58.3 ± 4.9	40.5 ± 3.4	45.6 ± 3.8	24.0 ± 2.7	0.4 (0)	0.6 (1)	0.5 (0)
19	37.9 ± 3.7	52.6 ± 6.0	53.5 ± 5.1	49.5 ± 3.9	1.3 (1)	0.9 (1)	0.9 (1)
20	24.5 ± 2.1	22.2 ± 2.0	38.9 ± 3.4	31.9 ± 3.4	1.3 (1)	1.4 (2)	0.8 (1)
21	65.8 ± 5.9	54.5 ± 4.2	78.1 ± 6.8	110.5 ± 13.4	1.7 (1)	2.0 (3)	1.4 (1)
22	22.5 ± 2.7	56.8 ± 6.1	49.5 ± 4.5	99.5 ± 7.4	4.4 (3)	1.8 (3)	2.0 (2)
23	30.0 ± 2.8	28.3 ± 3.2	28.5 ± 3.1	78.8 ± 6.8	2.6 (2)	2.8 (4)	2.8 (2)
24	42.5 ± 3.9	26.4 ± 2.7	20.9 ± 1.7	52.1 ± 6.2	1.2 (1)	2.0 (3)	2.5 (2)
25	27.2 ± 3.1	39.7 ± 4.0	46.2 ± 3.8	79.8 ± 8.1	2.9 (2)	2.0 (3)	1.7 (1)
26	38.8 ± 3.7	42.4 ± 4.3	41.4 ± 3.4	352.1 ± 40.0	9.1 (7)	8.3 (13)	8.5 (7)
27	46.6 ± 4.1	20.8 ± 2.3	25.6 ± 2.1	66.8 ± 8.1	1.4 (1)	3.2 (5)	2.6 (2)
28	26.6 ± 2.7	35.1 ± 3.1	30.6 ± 2.4	205.9 ± 17.0	7.7 (6)	5.9 (9)	6.7 (6)
29	36.5 ± 3.4	37.5 ± 4.0	19.1 ± 1.5	256.2 ± 22.8	7.0 (5)	6.8 (11)	13.4 (11)
30	21.4 ± 2.0	37.6 ± 4.2	65.5 ± 6.1	385.2 ± 31.9	18.0 (13)	10.3 (16)	5.9 (5)
31	33.4 ± 3.0	28.8 ± 2.4	54.1 ± 5.1	14.0 ± 1.1	0.4 (0)	0.5 (1)	0.3 (0)
32	15.4 ± 1.2	13.7 ± 1.1	46.2 ± 4.2	86.2 ± 7.8	5.6 (4)	6.3 (10)	1.9 (2)
33	85.2 ± 7.8	160.1 ± 14.8	53.1 ± 4.9	122.3 ± 13.8	1.4 (1)	0.8 (1)	2.3 (2)

34	25.3 ± 2.4	41.6 ± 3.8	37.1 ± 3.1	185.1 ± 21.6	7.3 (5)	4.5 (7)	5.0 (4)
35	21.6 ± 1.9	45.0 ± 4.2	29.0 ± 2.5	74.5 ± 8.7	3.4 (3)	1.7 (3)	2.6 (2)
36	45.5 ± 4.1	29.5 ± 3.4	29.1 ± 2.9	114.2 ± 12.9	2.5 (2)	3.9 (6)	3.9 (3)
37	34.2 ± 3.1	51.0 ± 4.5	41.5 ± 3.8	115.7 ± 11.0	3.4 (2)	2.3 (4)	2.8 (2)
38	39.5 ± 3.8	75.3 ± 6.4	46.2 ± 5.1	105.2 ± 9.1	2.7 (2)	1.4 (2)	2.3 (2)
39	27.6 ± 2.4	49.1 ± 4.2	66.7 ± 6.1	74.3 ± 6.9	2.7 (2)	1.5 (2)	1.1 (1)
40	42.0 ± 3.9	51.6 ± 5.4	55.5 ± 5.1	174.8 ± 15.6	4.2 (3)	3.4 (5)	3.2 (3)
41	23.8 ± 2.7	32.4 ± 3.4	15.5 ± 1.2	89.2 ± 7.4	3.8 (3)	2.8 (4)	5.7 (5)
42	36.9 ± 3.8	66.4 ± 5.9	60.3 ± 5.4	28.5 ± 3.1	0.8 (1)	0.4 (1)	0.5 (0)
43	24.3 ± 2.3	34.7 ± 3.8	43.0 ± 4.8	49.2 ± 3.8	2.0 (1)	1.4 (2)	1.1 (1)
44	52.7 ± 5.4	38.2 ± 4.1	39.1 ± 4.2	54.2 ± 5.0	1.0 (1)	1.4 (2)	1.4 (1)
45	13.5 ± 1.1	20.0 ± 1.4	15.1 ± 1.8	75.7 ± 6.9	5.6 (4)	3.8 (6)	5.0 (4)
46	85.4 ± 8.1	27.6 ± 2.8	52.6 ± 5.8	70.3 ± 7.2	0.8 (1)	2.5 (4)	1.3 (1)
47	51.2 ± 4.9	38.4 ± 3.7	86.3 ± 7.5	64.9 ± 5.7	1.3 (1)	1.7 (3)	0.8 (1)
48	42.2 ± 4.0	34.1 ± 3.9	61.8 ± 5.1	95.6 ± 8.6	2.3 (2)	2.8 (4)	1.5 (1)
49	41.1 ± 3.4	95.0 ± 8.7	52.1 ± 6.0	93.2 ± 7.4	2.3 (2)	1.0 (2)	1.8 (2)

[a]IC_{50} = the concentration required to give 50 % inhibition, calculated using GraphPad Prism. Each drug concentration was tested in triplicate in four separate determinations. [b]Towards Vero Cells after 72 h of culture. [c]Selectivity Index = IC_{50} Vero Cells/IC_{50} epimastigote form of parasite. In brackets: number of times that compound SI exceeds the reference drug SI (on epimastigote form of *T. cruzi*).

SI values higher than 10 in the epimastigote form, in any of the *T. cruzi* strains, were established as the cut-off in this first preliminary stage. Thus, compounds **6**, **7**, **9**, **10**, **29** and **30** were selected as potential trypanocidal agents. Subsequently, their activities were evaluated against the developed forms in vertebrate hosts (amastigote and trypomastigote forms), which are the relevant forms from the clinical perspective. The IC_{50} values and the SI for these selected compounds on extra- and intracellular forms of *T. cruzi* are shown in **Table 3** and **Table 4**, respectively. In accordance with some authors, potential antichagasic agents must meet certain criteria: IC_{50} value must not exceed 10 μM, and the SI must be higher than 50 [44]. Three out of the six tested compounds (**7**, **9** and **10)** fulfil those requirements at least for one of the parasite forms. Moreover, these three Mannich base-type derivatives showed IC_{50} values in Vero cells and SI that were superior to those of the reference

drug BZN. Therefore, these three compounds were prioritized to determine their *in vivo* trypanocidal activities. These *in vivo* assays were performed only in the *T. cruzi* Arequipa strain, as there were no significant differences between the performances of the selected compounds for the other evaluated strains.

Table 3. *In vitro* activity and cytotoxicity for selected compounds (**6, 7, 9, 10, 29** and **30**) on extra- and intracellular forms of *Trypanosoma cruzi.*

Comp	Activity IC_{50} (µM)[a] *T. cruzi* Arequipa strain			Activity IC_{50} (µM)[a] *T. cruzi* SN3 strain			Activity IC_{50} (µM)[a] *T. cruzi* Tulahuen strain			Toxicity IC_{50} Vero Cell (µM)[b]
	Epim. forms	Amast. forms	Trypom. forms	Epim. forms	Amast. forms	Trypom. forms	Epim. Forms	Amast. Forms	Trypom. forms	
BZN	16.9 ± 1.8	8.3 ± 0.7	12.4 ± 1.1	36.2 ± 2.4	16.6 ± 1.4	36.1 ± 3.1	19.7 ± 1.7	10.0 ± 0.8	15.1 ± 1.3	23.2 ± 2.1
6	28.4 ± 3.1	nd	nd	18.2 ± 1.4	24.0 ± 2.7	25.3 ± 2.1	46.2 ± 4.5	Nd	nd	234.6 ± 17.8
7	1.4 ± 0.1	0.6 ± 0.0	1.1 ± 0.1	2.0 ± 0.1	3.1 ± 0.3	1.4 ± 0.1	1.8 ± 0.2	1.6 ± 0.2	1.2 ± 0.1	55.0 ± 4.9
9	9.5 ± 0.8	3.6 ± 0.3	3.4 ± 0.3	6.3 ± 0.5	5.8 ± 0.5	3.9 ± 0.4	7.3 ± 0.6	3.8 ± 0.3	2.9 ± 0.3	300.0 ± 24.1
10	31.6 ± 0.3	29.4 ± 0.3	11.7 ± 0.1	22.0 ± 0.2	30.5 ± 0.3	3.1 ± 0.3	37.4 ± 0.4	33.6 ± 0.3	14.5 ± 0.1	587.2 ± 37.6
29	36.5 ± 3.4	nd	nd	37.5 ± 4.0	nd	nd	19.1 ±1.5	38.7 ± 3.4	32.1 ± 2.8	256.2 ± 22.8
30	21.4 ± 2.0	28.3 ± 2.7	31.6 ± 3.0	37.6 ± 4.2	51.1 ± 5.5	42.2 ± 4.1	65.5 ± 6.1	Nd	nd	385.2 ± 31.9

[a]IC_{50} = the concentration required to give 50 % inhibition, calculated using GraphPad Prism. Each drug concentration was tested in triplicate in four separate determinations. [b]Towards Vero Cells after 72 h of culture. nd, not determined.

Table 4. Selectivity Index for selected compounds (**6, 7, 9, 10, 29** and **30**) on extra- and intracelular forms of *Trypanosoma cruzi*.

Comp.	Selectivity index	Selectivity index	Selectivity index

	T. cruzi Arequipa strain [a]			*T. cruzi* SN3 strain [a]			*T. cruzi* Tulahuen strain [a]		
	Epim. forms	**Amast. forms**	**Trypom. forms**	**Epim. forms**	**Amast. forms**	**Trypom. forms**	**Epim. Forms**	**Amast. Forms**	**Trypom. forms**
BZN	1.4	2.8	1.9	0.6	1.4	0.6	1.2	2.3	1.5
6	8.3 (6)	nd	nd	12.9 (20)	9.8 (7)	9.3 (15)	5.1 (4)	nd	nd
7	40.2 (29)	88.7 (32)	49.1 (26)	27.9 (44)	17.6 (13)	39.9 (62)	30.2 (26)	34.6 (15)	47.4 (31)
9	31.5 (23)	82.4 (29)	89.6 (48)	47.8 (75)	51.5 (37)	76.1 (118)	40.9 (35)	78.7 (34)	102.7 (67)
10	18.6 (14)	20.0 (7)	50.4 (27)	26.7 (4)	19.2 (14)	187.0 (291)	15.7 (13)	17.5 (8)	40.6 (26)
29	7.0 (5)	nd	nd	6.8 (11)	nd	nd	13.4 (11)	6.6 (3)	8.0 (5)
30	18.0 (13)	13.6 (5)	12.2 (6)	10.3 (16)	7.5 (5)	9.1 (14)	5.9 (5)	nd	nd

[a]Selectivity index = IC_{50} Vero Cells/(IC_{50} extracellular and intracelular form of parasite. In brackets: number of times that compound SI exceeds the reference drug SI (on extracellular and intracellular forms of *T. cruzi*). nd, not determined.

From the structural perspective, it must be mentioned that the three lead compounds (**7**, **9** and **10**) presented the methoxy donor group substituted on the *para* position of the phenyl ring. The substitution of an extra methoxy group did not influence the cytotoxicity in Vero cells; however, this modification led to a reduction in *in vitro* activity and, as a consequence, a great decrement of the SI (compounds **7** vs. **11, 9** vs. **13 and 10** vs**. 14**). Furthermore, the substitution of the methoxy by the trifluoromethoxy moiety (compounds **7** vs. **46**, **9** vs. **48** and **10** vs. **49**) led to a clear increase in cytotoxicity and decrease in *in vitro* activity.

Ultimately, the rates of infection in host Vero cells were measured by counting the infected cells after 72 h of exposure at different concentrations to acquire more accurate information about the most active compounds, including BZN. The data are shown in **Figure 3**, together with the data of the amastigote and trypomastigote forms. The rates of infected cells gradually decreased in all cases, declining to 7 % for compound **7**, 15 % for compound **9** and 52 % for compound **10** at concentrations of 50 μM with respect to the infected control Vero cells. We must highlight the action of compounds **7** and **9**, with IC_{50} values (relative to the % of infected cells) of 1.9 μM and 6.4 μM, respectively. These two compounds showed higher efficiency than the reference drug BZN

(approximately 20 % of infected cells at 50 µM and with an IC_{50} value of 15.1 µM). Likewise, the average number of amastigote forms per cell decreased for all tested compounds (**Supplementary Figure S97**). A decrease in the number of amastigote and trypomastigote forms was also observed.

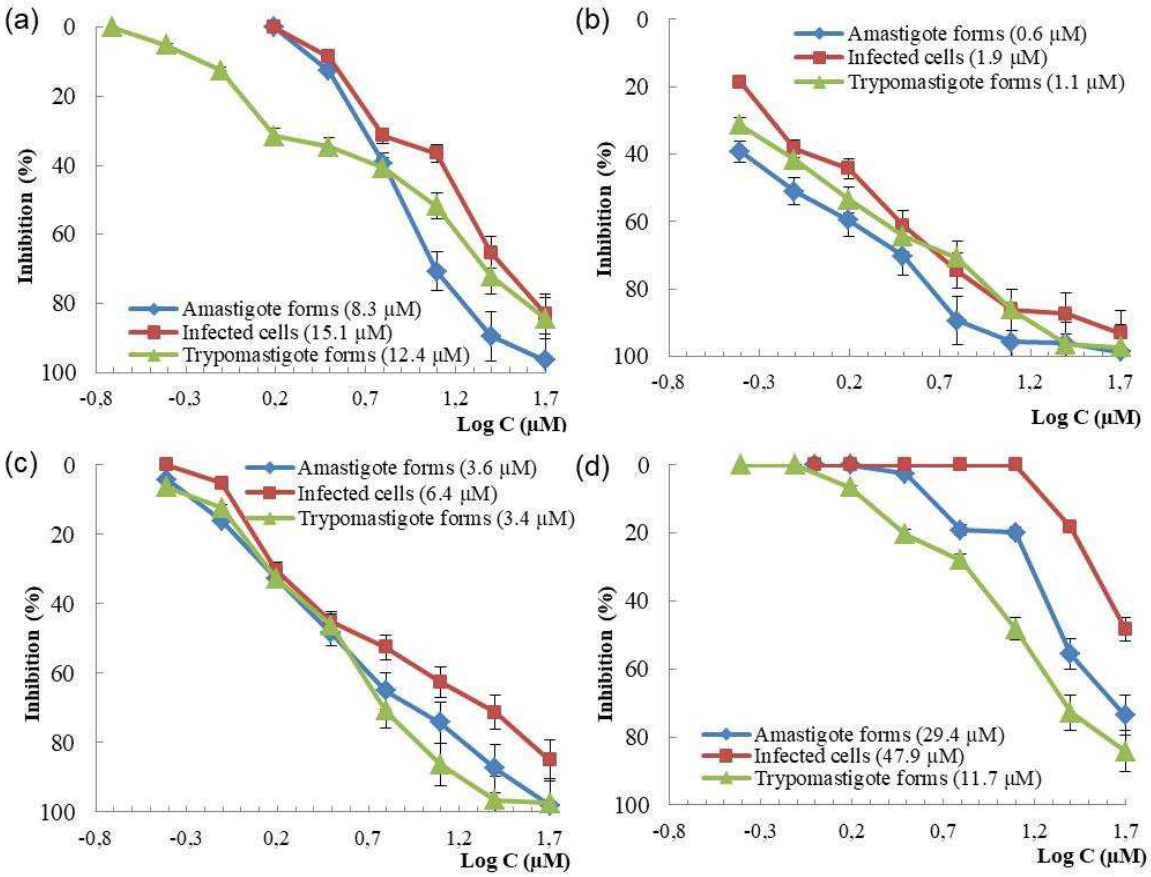

Figure 3. Reduction of the infection of *T. cruzi* Arequipa strain regarding the decrease of amastigote and trypomastigote forms and infected cells treated with (a) BZN, (b) **7**, (c) **9** and (d) **10**. Values are the means of the three separate determinations. In brackets: IC_{50} value, calculated using GraphPad Prism.

***In vitro* genotoxicity screening - SOS/umu assay.**

The SOS/umu genotoxicity assay has been used as a screening tool to determine the compounds to prioritize for further studies. The three most active compounds in the *in vitro* evaluation (compounds **7**, **9** and **10**) were included in the SOS/umu test to explore their genotoxicity. All

assessed compounds were non-genotoxic with or without metabolic activation in the tested conditions (supp. Material). However, BZN showed *in vitro* genotoxicity with and without metabolic activation. The obtained results confirm the promising profile of these series.

***In vivo* anti-*T. cruzi* activity in BALB/c female mice.**

To assess the effectiveness of the treatment in both the acute and chronic phases, experimental tests during the *in vivo* evaluation were performed to examine the following: a) parasitaemia levels by counting bloodstream trypomastigotes in the acute phase treatment; b) parasitaemia reactivation in the chronic phase by counting bloodstream trypomastigotes after immunosuppression (IS); c) parasites in target organs in the chronic phase by PCR after IS; d) levels of immunoglobulin-G (Ig-G) by the enzyme-linked immunosorbent assay (ELISA) and the splenomegaly as indicators of the immune response; e) serum biochemistry parameters as an indicator of metabolic disturbances or abnormalities related to the treatment.

Since compounds **7**, **9** and **10** exhibited remarkable *in vitro* results towards trypomastigote and amastigote forms (IC_{50} and SI values close to the criteria established by Nwaka et al. [44]) and the screening test showed no genotoxicity, those Mannich base-type derivatives were evaluated in BALB/c mice (*in vivo* studies).

As mentioned above, and because of the different effectiveness levels of current drugs in the treatment against CD during the acute and chronic phases (where the performance of drugs is not as effective as it should) [45], the effect of these compounds was evaluated by treating mice in each phase: the treatment was carried out from day 10 post-infection (pi) for the acute phase and from day 75 pi (it was established that the animals entered the chronic phase, in which there are no parasites remaining in the bloodstream) for the chronic phase, both during 5 consecutive days. Drugs were administered by oral dose because it is the preferred route for the treatment of parasitic diseases, in addition to the oral therapeutic route, which leads to better patient compliance and has a low cost (critical aspects of human treatment in developing countries) [46].

Treatment for both compounds under study and the reference drug BZN was performed with subcurative doses for BZN (20 $mg \cdot kg^{-1}$ per day for 5 days) to evaluate whether the compounds demonstrated higher *in vivo* effectiveness than the reference drug. Noticeably, none of the treated mice died during and/or after treatment, nor did they lose more than 10 % body mass. Those compounds with higher effectiveness could be studied at higher doses since they do not present toxicity, establishing a new treatment guideline based on pharmacokinetic studies, to achieve total cure. It is proposed that the different effectiveness levels in the acute and chronic phases are related to inadequate pharmacokinetics between the compounds and the location of the parasites in the tissues during the chronic phase of infection [47].

First, **Figure 4** shows the parasitaemia levels in the different groups of mice that were untreated and treated in the acute phase. A reduction of parasitaemia in mice treated with the tested Mannich base-type derivatives with respect to the untreated mice was observed. Moreover, compound **9** exhibited higher *in vivo* trypanocidal activity in the acute phase than the reference drug BZN. This activity was evident since the beginning of the treatment (day 10 pi) and was maintained until the end of the acute phase (day 50 pi). The peak of parasitaemia (day 23 pi) caused a reduction of 68 % for compound 10, 76 % for compound 9 and 55 % for compound 7, compared with the control group; even compound 9 showed a higher reduction than BZN (76 % versus 70 %, respectively). Furthermore, parasitaemia was not detected on day 40 pi for compound **9**, while it was observed in the group of mice that were untreated and treated with BZN up to day 49 and 47 pi, respectively. This finding appears to indicate that parasites were eliminated or were depleted to undetectable levels for counting.

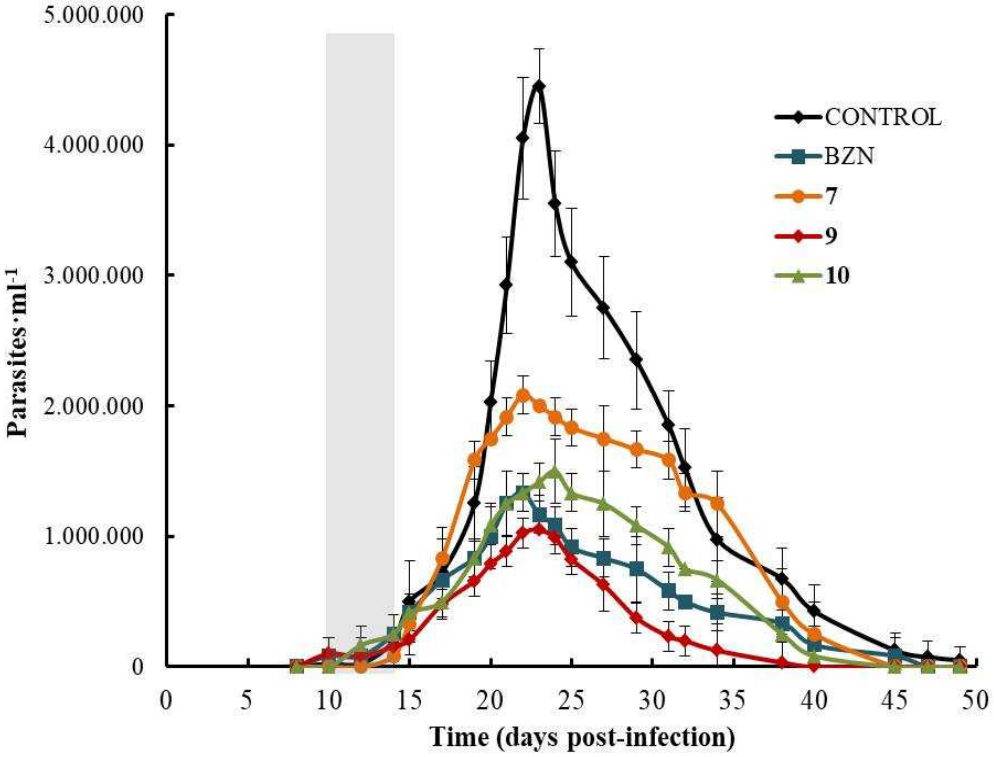

Figure 4. Parasitaemia in murine model of acute CD: control (untreated), BZN, compound **7**, compound **9** and compound **10**. In all cases, mice were intraperitoneally infected with trypomastigotes of *T. cruzi* Arequipa strain, and compounds were orally administered with a total dose of 100 mg·kg^{-1} of body mass. Treatment days are represented in grey. Values constitute means of six mice ± standard deviation.

Second, with the aim of determining the effectiveness of the treatment and the disease extent in the chronic phase, parasitaemia reactivation was determined after IS up to day 120 pi (late chronic phase, when the parasite is nested inside target organs in the amastigote form), as mentioned in the experimental section. The objective was to reactivate the parasitaemia under the control of the immunological system of mice, which was blocked using cyclophosphamide monohydrate (CP). The reactivation is an important matter because seemingly cured immunocompromised individuals and cured patients submitted to kidney or liver transplantation (treated with anticancer chemotherapy or diagnosed with AIDS) exhibit clinically aggressive reactivation of the parasitaemia. Hence, IS is performed as a first cure confirmation technique, with the second being

PCR of the organs (which is mentioned below): those animals infected with *T. cruzi* and treated with parasitaemia that does not reappear and negative PCR results for organs after IS are considered cured [48]. **Figure 5** shows the percentage of reactivation of parasitaemia after IS in comparison with the control groups, which is proportional to the survival rate of the parasites. Parasitaemia reactivation was reduced for all mice treated with the tested compounds and with BZN in both the acute and chronic phases. It is noteworthy that all tested compound-treated mice in the acute phase showed reduced parasitaemia reactivation than those treated in the chronic phase; the opposite occurred for mice treated with BZN. Regardless, compound **9**-treated mice showed the lowest reactivation of parasitaemia both in the acute and chronic phases (12 % and 20 %, respectively), even with much lower values than those mice treated with BZN (75 % and 51 %, respectively). This significant decrease in parasitaemia reactivation was expected in compound **9**-treated mice in the acute phase because of the obtained parasitaemia curve (mentioned above). Additionally, as mentioned below, the presence of parasites in the target organs was negative for most of the analysed organs in these mice treated in the acute phase. Moreover, the low parasitaemia reactivation observed in compound **9**-treated mice in the chronic phase indicated that the treatment was also effective in this phase and confirmed the results obtained using PCR.

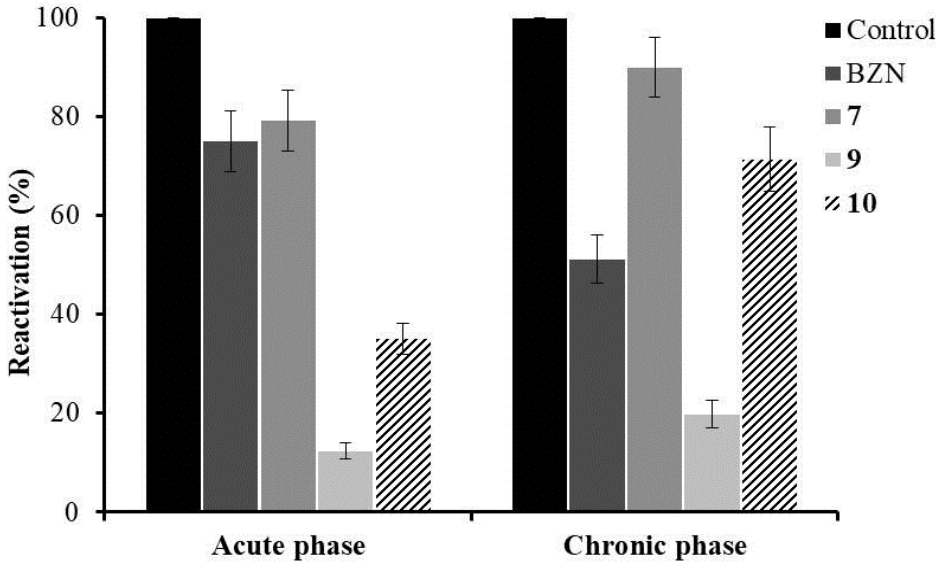

Figure 5. Immunosuppression *in vivo* assay for mice untreated (control) and treated with BZN, **7, 9** and **10**. Figure shows the reactivation of parasitaemia after the treatment in both phases and the immunosuppression cycles by fresh blood in comparison to the mice untreated (control). Values constitute means of six mice ± standard deviation.

Finally, the presence of parasites in the target organs was determined by PCR after necropsy (day 127 post-infection) to evaluate the curative effect of these compounds as a second technique of confirmation of cure. PCR results for the target organs (positive for control groups) in the different groups of mice, both treated in the acute phase and in the chronic phase, are shown in **Figure 6**. PCR of the control groups, both in the acute and chronic phases, was positive for these 9 organs and tissues: adipose, bone marrow, brain, oesophagus, heart, lung, muscle, spleen and stomach. As observed and according to previous studies, compound **9** showed the best *in vivo* trypanocidal activity, which was even better than that shown by the reference drug BZN: 89 % and 78 % of parasite-free organs/tissues for compound **9**-treated mice in the acute and chronic phases, respectively, in comparison with BZN-treated mice (33 % and 55 % of parasite-free organs/tissues), thus confirming the partial curative effect of this compound at this dosage in both phases.

Assessment of clinical cure in *T. cruzi* infections is debatable due to the lack of a trustworthy test to ensure parasite elimination [49]. PCR techniques to identify cure raise critical questions, and their main utility is to confirm the failure of clinical cure because even consistently negative results using blood, for which this technique is capable of detecting a single parasite in 5 mL, are insufficient to confirm the complete elimination of tissue parasites [50, 51]. Detection methodology has been enhanced by specific PCR with the TaqMan technology, using fluorogenic probes, real-time amplification reaction and sequences of constant regions and variables of minicircles of kinetoplast DNA. This technology is quite useful to assess the parasitic load in earlier and later-treated chronic patients and for the future establishment of a suitable criterion for the healing of patients submitted to therapy [52]. Regarding animal testing models, IS is the formula applied to demonstrate cure [53]. We

evaluate the establishment of cure in the chronic phase, as mentioned above, using a double confirmation based on IS and PCR of the target organs after necropsy. Therefore, we evaluate the presence (or not) of parasites in both blood and tissue. At present, highly sensitive bioluminescence imaging model techniques are used to prove cure, generating data with superior accuracy to other methods, including PCR [53]. However, we can provide evidence of cure (or, at least, a considerable reduction in the parasitic load) based on the results of six independent samples by PCR and reactivation after IS (double checking of cure).

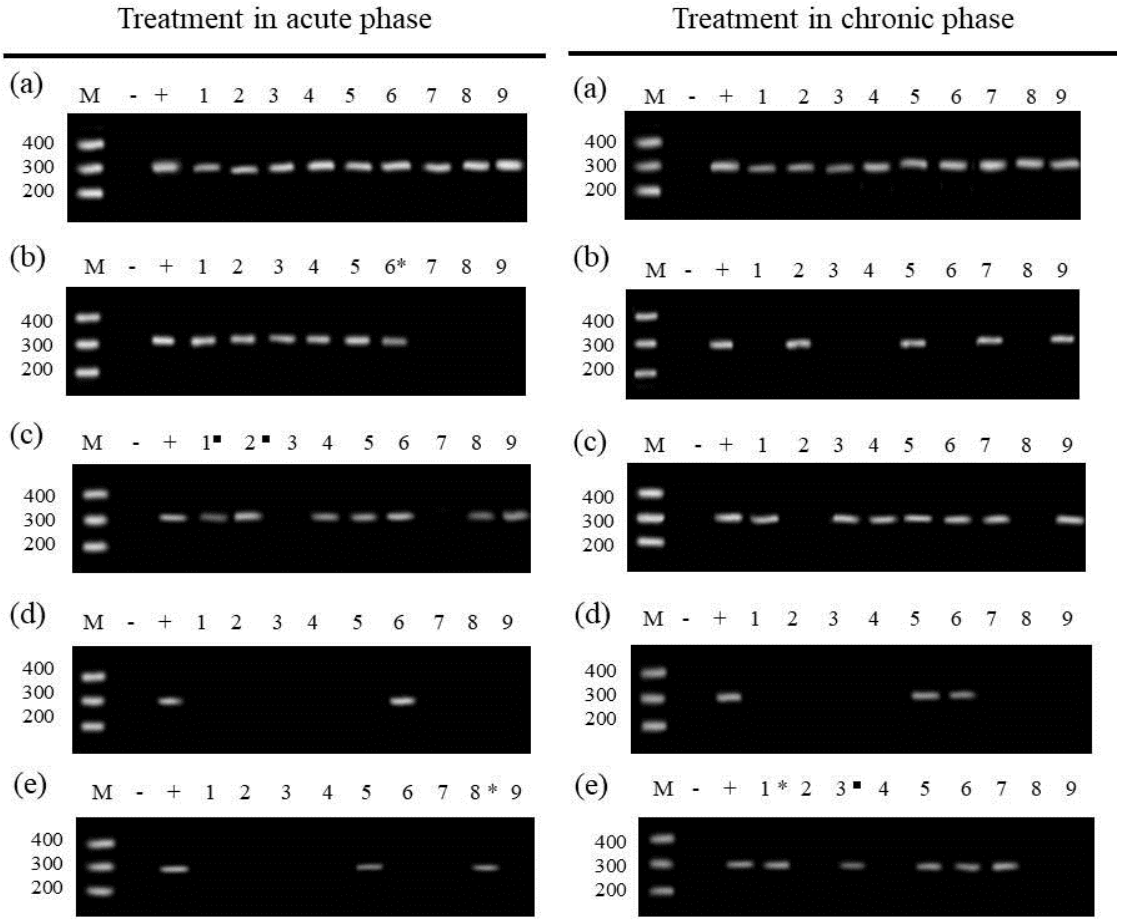

Figure 6. PCR analysis of 9 tissues with the *T. cruzi* SOD gene at the final day of experiment in mice untreated and treated with 100 mg·kg^{-1} body mass. (a) Shows untreated mice group, (b) Shows the group of mice treated with BZN, (c) Shows the group of mice treated with **7**, (d) Shows the group of mice treated with **9**, (e) Shows the group of mice treated with **10**. Lanes: M, base pair (bp)

marker; -, PCR negative control; +, PCR positive control; 1, PCR adipose tissue; 2, PCR bone marrow tissue; 3, PCR brain tissue; 4, PCR oesophagus tissue; 5, PCR heart tissue; 6, PCR lung tissue; 7, PCR muscle tissue; 8, PCR spleen tissue; 9, PCR stomach tissue. *, It means that 2/6 of the corresponding organ PCR products showed 300 bp band on electrophoresis; ▪, It means that 4/6 of the corresponding organ PCR products showed 300 bp band on electrophoresis; no *▪, it means that 6/6 or 0/6 of the corresponding organ PCR products showed 300 bp band on electrophoresis.

To assess the immune status of the mice (untreated and treated in different phases) during infection, Ig-G levels were determined using the ELISA and Fe-SOD enzyme (isolated in our laboratory) like antigen [54]. Detection of total Ig-G reveals the infection rates and verifies the level of protection (effectiveness) attributed to the tested compounds, in combination with the innate protection of mice, because the titre of immunoglobulins is linked to the parasite load [55]. **Figure 7** shows the titre of anti-*T. cruzi* Ig-G. All treated mice and samples analysed in the acute and chronic phases showed decreased Ig-G levels with respect to samples from untreated (control) mice, excluding those of day 81 pi in the chronic phase, which is rational since those samples were retrieved from mice only two days after treatment. Mice treated with compounds **7** and **10** showed higher Ig-G levels than those that received reference drug BZN in both acute and chronic phases, suggesting a higher parasitic load and a lower trypanocidal effect, consistent with previous studies. In contrast, compound **9**-treated mice showed a significant reduction of Ig-G levels and the lowest increase in these levels after IS as a consequence of the low parasitaemia and the low reactivation after IS, mainly due to the good *in vivo* trypanocidal activity of this compound, as demonstrated by PCR.

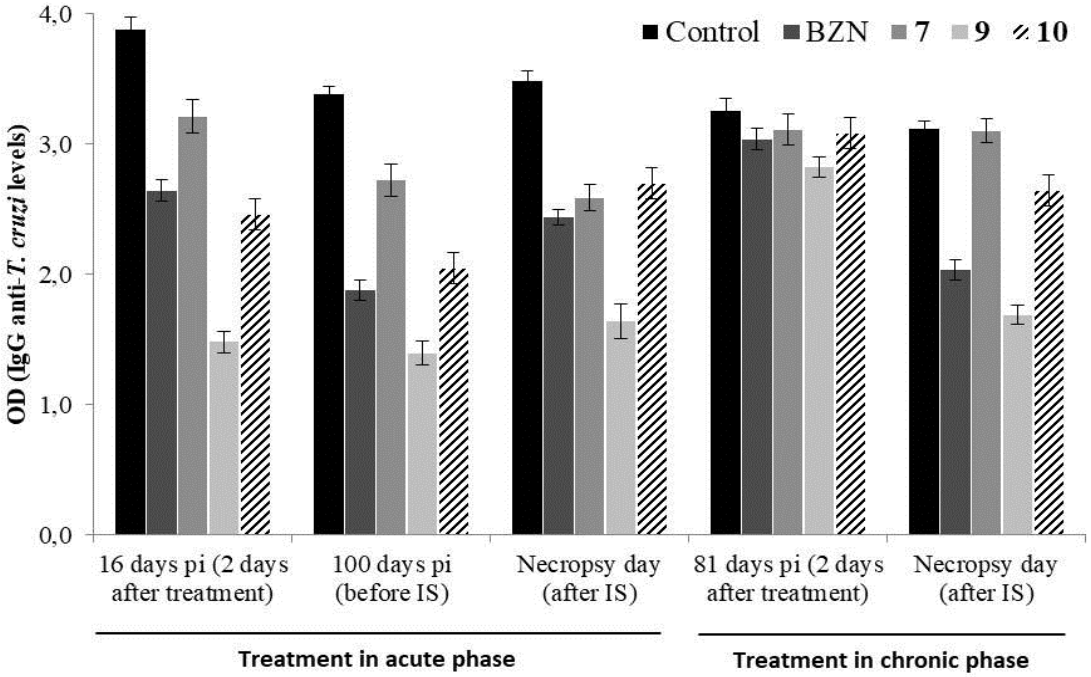

Figure 7. Differences in the Ig-G levels of anti-*T. cruzi* antibodies, expressed in absorbance units (optical densities (OD) at 490 nm), between control (untreated) and treated groups of mice at different days post-infection (pi). IS, immunosuppression.

Another feature that is linked to the parasite load is splenomegaly, since the spleen is an organ that is implicated in defence against infection. Splenomegaly occurs in experimentally infected mice in both acute and chronic phases, during which the spleen of chronic mice is frequently approximately twice the mass of those from uninfected mice [53]. Importantly, treatment with BZN reduces infection-induced splenomegaly, even at subcurative doses and in the absence of parasitological cure, since it is linked to a reduction of the parasite load [53]. Accordingly, **Figure 8** shows the weight percentage of spleens from different groups of mice in both acute and chronic phases. We found that untreated (control) mice showed a weight percentage value that was twice the value corresponding to uninfected mice: 0.28 % for uninfected mice and 0.56 % and 0.59 % for untreated (control) mice in the acute and chronic phases, respectively. Moreover, untreated mice showed a higher weight percentage value in both phases compared with the mice treated with the tested compounds and BZN. This finding indicated that the tested Mannich base-type derivatives

and BZN reduced splenomegaly and, therefore, infection rates. Compound **9**-treated mice showed lower splenomegaly: these mice showed a reduction of splenomegaly of 52 % for mice treated in the acute phase and 68 % for mice treated in the chronic phase compared with untreated mice. It should be mentioned that the higher splenomegaly usually observed in the mice treated in the chronic phase should not be related to a lower activity in this phase; these mice simply suffered an acute phase without treatment with high levels of parasitaemia.

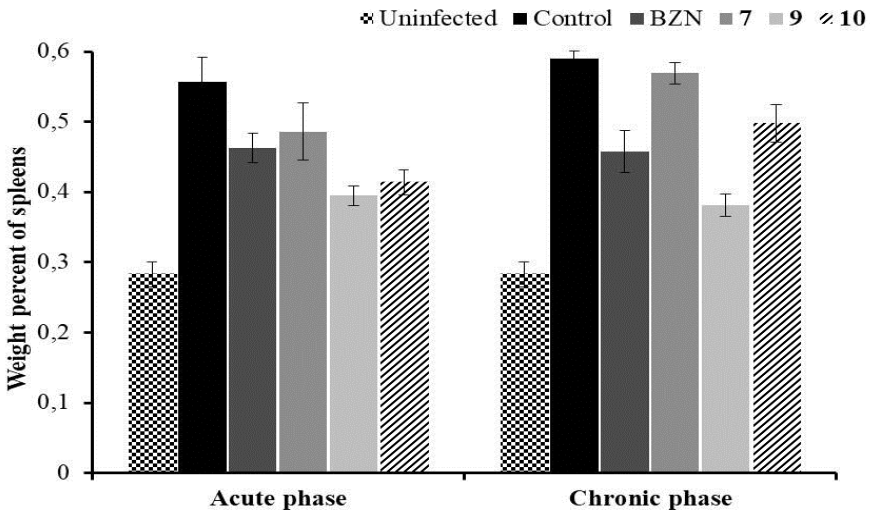

Figure 8. Weight percent of spleens of different groups of mice at the final day of experiment. Values constitute means of six mice ± standard deviation.

To confirm the metabolic abnormalities associated with the treatment, clinical chemistry measurements were carried out as mentioned in the experimental section. **Table 5** shows the biochemical clinical parameters obtained in both untreated and treated mice in the acute and chronic phases, where values for uninfected and untreated mice were also included. Most of the biochemical parameters tested for the three studied compounds were not altered after compound administration, and almost all those alterations returned to normal levels in the samples obtained on the day of mice necropsy. Moreover, these tested compounds showed less toxicity than the reference drug BZN. The lack of toxicity along with the high activity of compound **9** led us to consider this compound as a promising candidate for the treatment of CD.

Table 5. Biochemical clinical parameters measured at different experimental situations and days post-infection (pi) in groups of BALB/c mice infected with *T. cruzi*.

		Group	Kidney marker profile		Heart marker profile		Liver marker profile			
			Urea (mg/DL)	Uric acid (mg/DL)	CK-MB[a] (U/L)	LDH[b] (U/L)	AST/GOT[c] (U/L)	ALT/GPT[d] (U/L)	Total bilirubin (mg/DL)	Alkaline phosphatase (U/L)
		Uninfected mice (n = 15)	35 [32-40]	4.5 [4.0-5.1]	372 [150-630]	3180 [2505-3851]	153 [132-177]	55 [46-62]	0.28 [0.22-0.31]	169 [141-192]
Treatment in acute phase	16 days pi*	control	31	4.3	535	3275	167	60	0.23	180
		BZN	---	----	=	=	++++	++++	++	++
		Compound **7**	+++	++	=	=	---	---	-	--
		Compound **9**	---	---	--	--	--	--	-	-
		Compound **10**	--	--	=	=	++++	++++	=	=
	Necropsy day	control	34	4.0	496	2761	179	49	0.21	161
		BZN	---	=	=	=	++++	=	+	=
		Compound **7**	+	+	=	=	-	=	=	=
		Compound **9**	=	=	=	=	-	-	=	=
		Compound **10**	=	=	=	=	+++	+++	=	=
Treatment in	81 days pi*	control	45	5.7	751	5951	260	57	0.25	167

chronic phase		BZN	---	----	--	---	++	++	+++	++++
		Compound **7**	+++	+	-	-	---	---	-	-
		Compound **9**	---	---	---	--	--	---	--	=
		Compound **10**	-	---	--	=	+++	+++	=	+
	Necropsy day	control	37	4.8	538	6679	286	64	0.20	149
		BZN	---	--	=	--	+	=	++	++
		Compound **7**	+	=	=	=	--	-	=	=
		Compound **9**	=	=	-	=	--	-	=	=
		Compound **10**	-	---	=	=	++	+	=	=

*2 days after treatment. [a]CK-MB, creatine kinase-muscle/brain. [b]LDH, lactate dehydrogenase. [c]AST/GOT, aspartate aminotransferase. [d]ALT/GPT, alanine aminotransferase. pi, post-infection.

Key: =, variation no larger than 10 %; +, up to 10 % increase over the range; ++, up to 20 % increase over the range; +++, up to 30 % increase over the range; ++++, more than 40 % increase over the range; −, up to 10 % decrease over the range; − −, up to 20 % decrease over the range; − − −, up to 30 % decrease over the range; − − − −, more than 40% decrease over the range.

Metabolite excretion.

T. cruzi catabolizes glucose at a high rate, excreting into the medium a substantial portion of the hexose skeleton as partly oxidized end products [56], and acidifying the medium in the presence of oxygen [57, 58]. The final products in this catabolism are mainly pyruvate, acetate, succinate, L-alanine, D-lactate and ethanol [59].

Proton nuclear magnetic resonance (^{1}H NMR) spectra of treated and untreated *T. cruzi* Arequipa epimastigotes forms were registered to obtain some information about the effects of compounds **7**, **9** and **10**, at IC_{25} concentrations, on glucose metabolism in *T. cruzi* (spectra not shown). The final excretions were qualitatively and quantitatively analysed and compared with those found for the control (untreated *T. cruzi* epimastigotes). **Figure 9** shows the results obtained compared with this control. The most remarkable differences were the altered amount of succinate, with value changes higher than 20 % for the three tested Mannich base-type derivatives. It is interesting to note the effect of compound **9**, which showed an increase in succinate excretion of 200 %. Non-significant alterations were observed in the other metabolites. It is well-known that the increase in the amount of succinate indicates catabolic changes that could be associated with a mitochondrial malfunction due to the redox stress produced by inhibition of the mitochondrion-resident Fe-SOD enzyme [60], and not by a direct effect on the glycolytic pathway. Owing to the feasible mitochondrial dysfunction and that the main role of succinate is to maintain the glycosomal redox balance via NADH reoxidation produced in the glycosome catabolic pathway, it is possible that this route can be increased to maintain the balance, with the consequent increase in succinate as the final product [57, 61]. In contrast, compound **7** produces a reduction in succinate excretion along with a reduction of pyruvate and increase in glycerol. These results suggest, in addition to alterations at the mitochondrial level, that some of the glyceraldehyde-3-phosphate pathway-involved enzymes of glucose catabolism (like glyceraldehyde-3-phosphate

dehydrogenase or phosphoglycerate kinase enzymes) can be inhibited and the carbon skeleton directed towards the glycerol pathway as the final product [57].

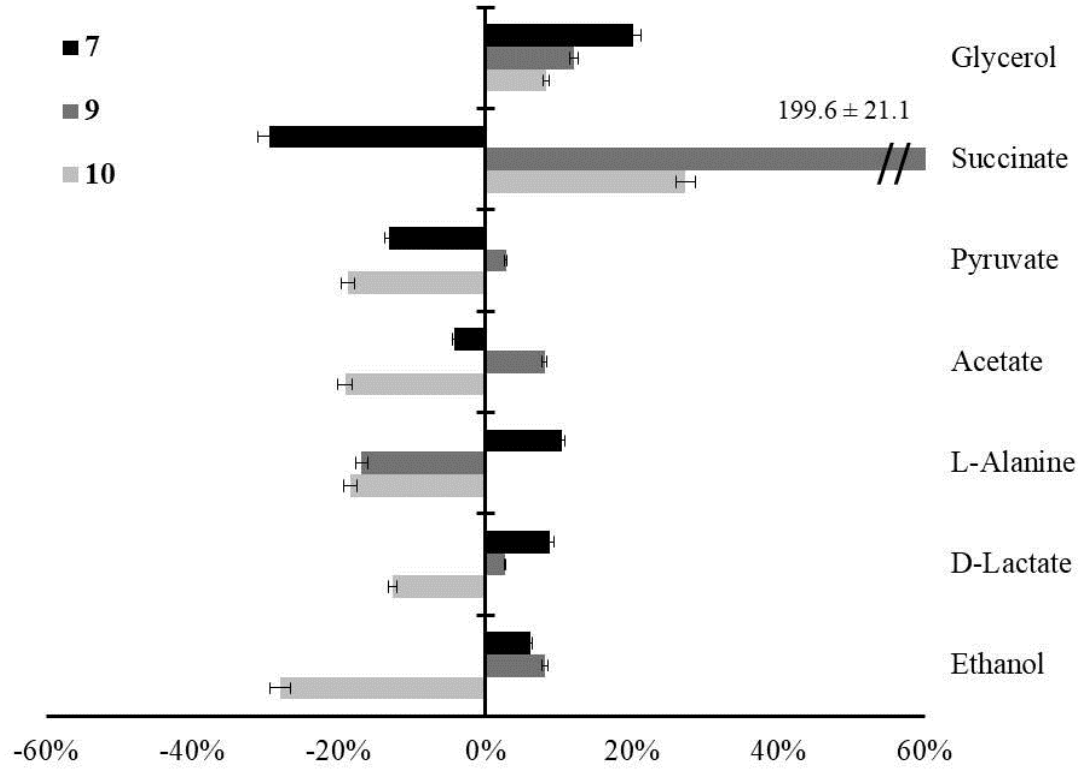

Figure 9. Percentages of variation among peaks of catabolites excreted by epimastigotes of *T. cruzi* Arequipa strain exposed to compounds **7**, **9** and **10** at their IC_{25} in comparison to a control (untreated) incubated 72 h. Each drug was tested in three separate determinations.

Effects on the mitochondrial membrane potential and DNA replication and RNA synthesis in *T. cruzi.*

It is well-known that mitochondria play an imperative role in cell death decisions. In normal cells, active pumping of H^+ is produced to maintain the electrochemical gradient and the integrity and function of mitochondria. Disturbances in this potential lead to a decrease in ATP production and a reduction in DNA replication and RNA transcription [62, 63].

As mentioned above, *T. cruzi* catabolizes glucose at a high rate through the pentose phosphate pathway (PPP). Subsequently, these metabolites are directed to the tricarboxylic acid (TCA) cycle in the mitochondria for ATP synthesis, along with the electron-transport chain [64]. Mitochondrial dysfunction can then produce an imbalance in the ATP/ADP and NADH/NAD^+ ratios, in addition to a cellular accumulation of pyruvate, malate and succinate, causing a blockade of the glycolytic pathway [57]. BZN, for instance, kills *T. cruzi* through its reduction by type I nitroreductase activity that leads to the formation of highly reactive metabolites [65]: it causes respiratory chain inhibition, and thus we observed a decrease in mitochondrial membrane potential when treating *T. cruzi* with BZN.

Therefore, to evaluate whether the alteration observed in glucose metabolism pathway in the metabolite excretion study was a consequence of a mitochondrial dysfunction (and not a direct action of the tested compounds at the glycosome or cytoplasmic level), studies were conducted on this organelle using rhodamine 123 (Rho 123) and acridine orange (AO).

Figure 10 shows the results of the flow cytometry analysis of the mitochondrial membrane potential. We observed a membrane potential reduction by 35.4 % when *T. cruzi* was treated with BZN, which causes respiratory chain inhibition. Cells treated with compounds **7** and **9** and labelled with Rho 123 showed a decrease in membrane potential with an approximate value of 26 %, whereas the highest depolarization of the mitochondrial membrane occurred in compound **10**-treated cells (76.3 %). These alterations could precede *T. cruzi* cell death via necrosis in a mitochondrion-dependent manner, which could be the cause of their trypanocidal activities.

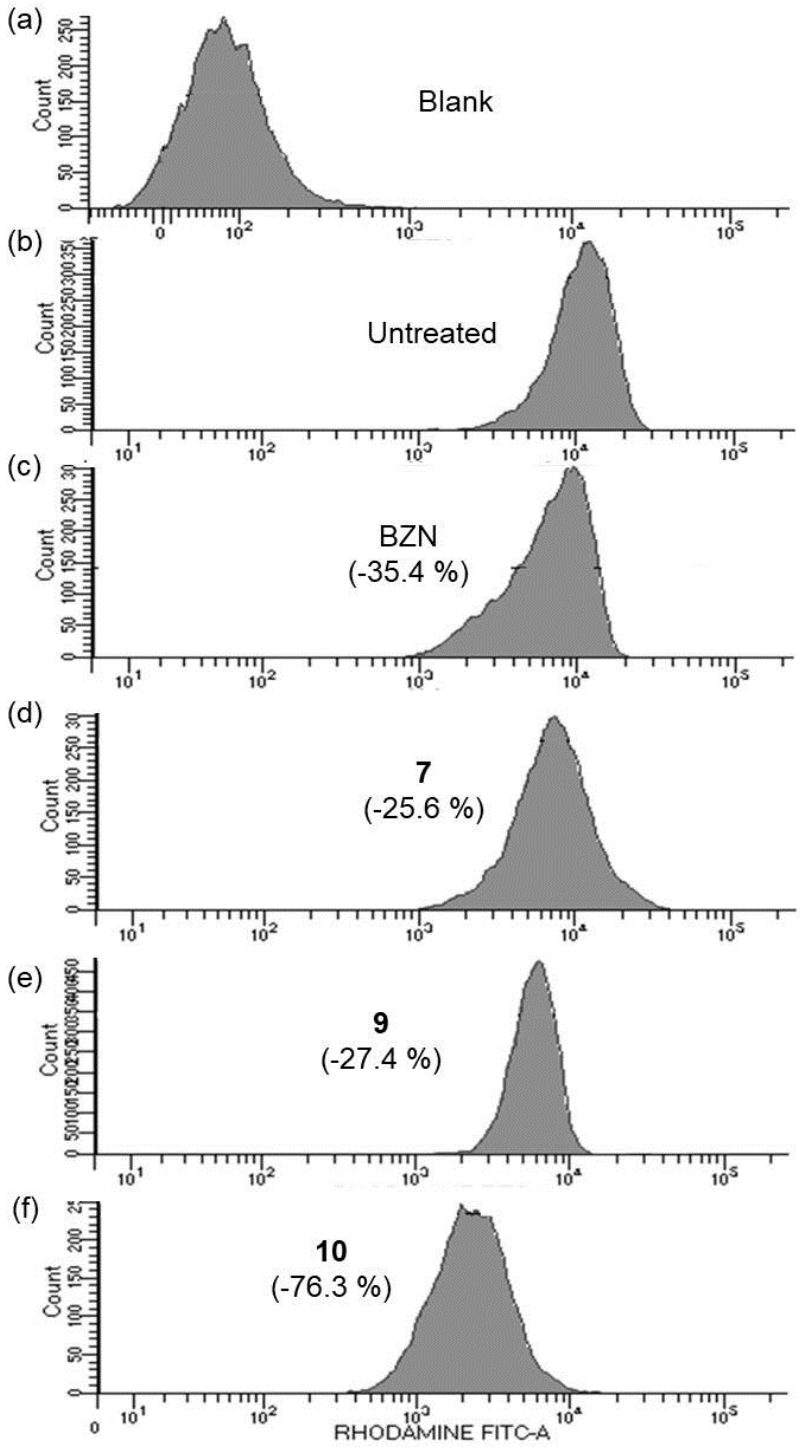

Figure 10. Cytometry analysis of the mitochondrial membrane potential from epimastigotes of *T. cruzi* Arequipa strain exposed to BZN and compounds **7**, **9** and **10** at their IC_{25} in comparison to a control

(untreated) incubated 72 h: (a) blank, (b) control (untreated), (c) BZN, (d) **7**, (e) **9** and (f) **10**. In brackets: percentage of alteration in mitochondrial membrane potential.

To determine whether the disturbances in the mitochondrial membrane potential caused a decrease in ATP production affecting DNA replication and RNA transcription, fluorescence intensities of AO of treated and untreated parasites were registered. The results are shown in **Figure 11**. All compounds and the reference drug BZN showed a decrease in the AO fluorescence intensity. BZN and compounds **7** and **9** caused similar values in terms of the reduction in the amount of DNA and RNA (between 18 % and 25 %); however, compound **10**-treated cells showed a considerable reduction, with an inhibition value of 72.9 %. A close relationship between the membrane depolarization and the amount of DNA and RNA was observed because compound **10** is also the Mannich bases-type derivative with the highest effect on mitochondrial membrane depolarization. It must be mentioned that this decrease in DNA and RNA was also due to random nucleic acid degradation (a feature commonly attributed to cell necrosis) and not only because of the ATP deficit [66].

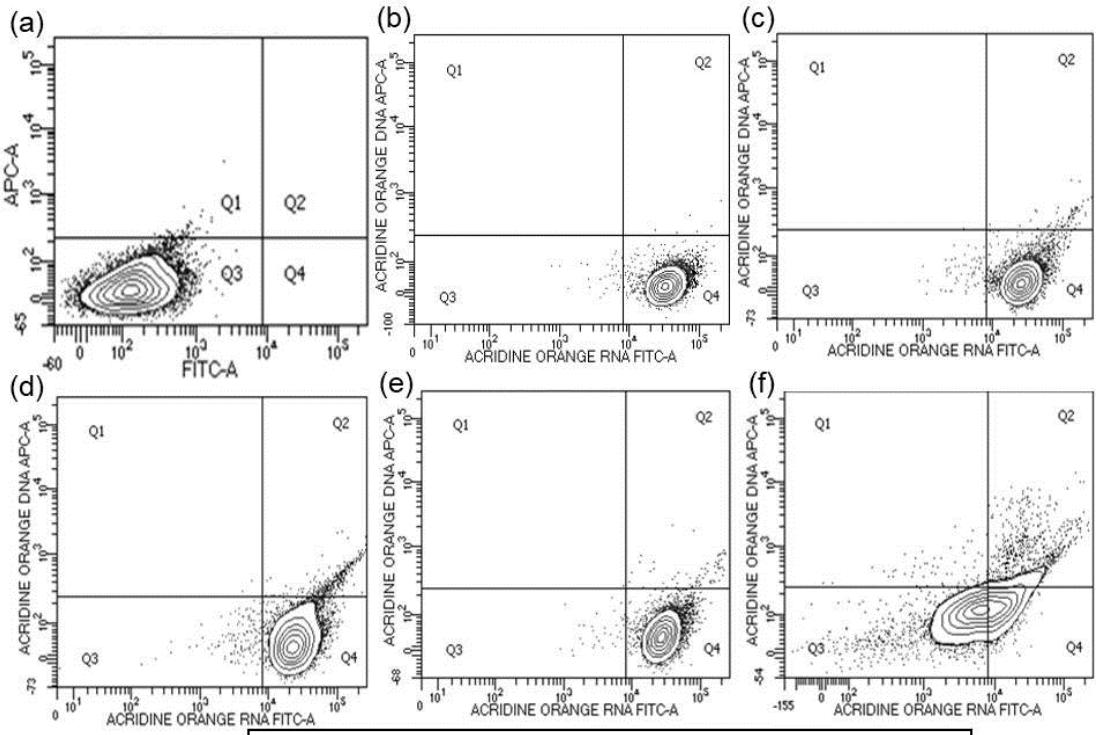

Compound	BZN	**7**	**9**	**10**
Inhibition (%)	22.4	24.6	18.0	72.9

Figure 11. Cytometry analysis of the inhibition in DNA replication and RNA synthesis of epimastigotes of *T. cruzi* Arequipa strain exposed to BZN and compounds **7**, **9** and **10** at their IC_{25} in comparison to a control (untreated) incubated 72 h: (a) blank, (b) control (untreated), (c) BZN, (d) **7**, (e) **9** and (f) **10**.

As mentioned above, the alteration in succinate excretion observed in the metabolite excretion study could be associated with mitochondrial dysfunction due to the redox stress produced by inhibition of the mitochondrion-resident Fe-SOD enzyme [60]. Therefore, to check if the final cause of the metabolic alteration and mitochondrial dysfunction was due to the inhibition of this enzyme, we studied the inhibitory effect of these Mannich base-type derivatives on *T. cruzi* Fe-SOD enzyme.

Inhibitory effect on the *T. cruzi* Fe-SOD enzyme.

Enzymes are one of the most studied therapeutic targets, and the trypanosomatid Fe-SOD is a trypanosomatid exclusive enzyme and absent in other eukaryotic cells [67, 68]. It presents biochemical and

structural differences with respect to its human homologue Cu/Zn-SOD. Elimination of reactive oxygen species (ROS), allowing trypanosomatids to protect themselves from the damage produced by oxidative stress, is a crucial role performed by this enzyme [69, 70]. Therefore, this Fe-SOD has been given special importance.

The trypanocidal activity of previous Mannich base-type derivatives has been partly explained by their inhibitory effects on *T. cruzi* Fe-SOD, and thus the possible action of these new molecules on the enzyme was evaluated [32]. The effect of the studied compounds on Fe-SODe and CuZn-SOD activities was determined at concentrations of 1-100 μM using the method described by Beyer and Fridovich [71].

Figure 12 shows the inhibition data obtained for compounds **7**, **9** and **10**, with the corresponding calculated IC_{50} for Cu/Zn-SOD from human erythrocytes and Fe-SOD from *T. cruzi*. Significant inhibition values were found for the parasite enzyme, with IC_{50} values of 7.8 μM, 6.5 μM and 5.0 μM for compounds **7**, **9** and **10**, respectively, and 100 % inhibition at 50 μM. Furthermore, the three tested compounds showed no inhibitory activity against the human enzyme. Therefore, we have found effective potential drugs that are remarkable selective inhibitors of Fe-SOD. We suggest that this Fe-SOD enzyme be considered one of the targets of these compounds, and modelling studies are presented below to further investigate this point. In addition, this significant inhibitory effect could be the final cause of the mitochondrial dysfunction and the trypanocidal activity of these compounds because the SOD enzyme is an essential component of the mitochondrial redox stress response [72]. In contrast, the possibility of a multitarget compound should not be discarded.

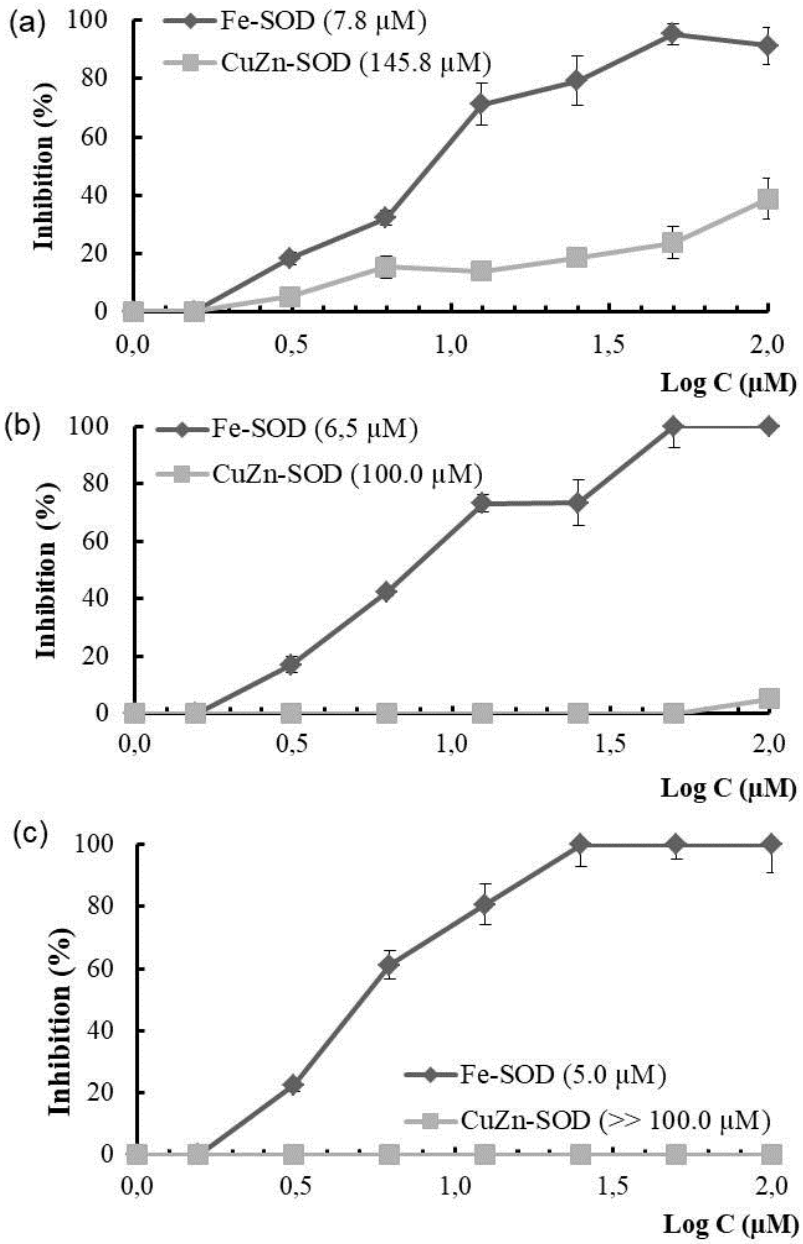

Figure 12. *In vitro* inhibition of Fe-SOD from epimastigotes of *T. cruzi* Arequipa strain (activity 42.0 ± 3.8 $U \cdot mg^{-1}$) and of CuZn-SOD from human erythrocytes (activity 47.3 ± 4.1 $U \cdot mg^{-1}$) for compounds (a) **7**, (b) **9** and (c) **10**. Activity differences in the control vs. the sample incubated using compounds were identified by the Newman-Keuls test. Values are the average of three separate rate determinations. In brackets: IC_{50} value, calculated by linear regression analysis.

Docking study of the new compounds with the *T. cruzi* Fe-SOD enzyme.

Docking studies with the parasite Fe-SOD enzyme were performed for the three best compounds, **7**, **9** and **10**, as well as for other ligands of this series (**1, 3, 8, 14, 17, 26, 31, 33, 38, 42, 47**) to cover a broader spectrum of structural variability, with the objective of analysing their binding mode and supporting the future design of more potent anti-Chagas agents as Fe-SOD inhibitors. The chemicalize web server predicted a pKa close to 7.4 for the piperazine nitrogen atom closer to the carbonyl group (in bold in **Figure 1B**), and therefore docking was performed both for the protonated and the neutral forms. The obtained binding mode is exemplified in **Figure 13A** for the protonated form of compound **9**. In general, the binding mode was found to be conserved between the compounds, such as between the two protonation states tested, even if the protonated ligands displayed a generally higher binding energy (*See Supplementary Figure S98A and Supplementary Table S3)*. Moreover, these compounds presented the same binding mode observed in a previous series published by our group [21]. Similarly, as observed in our previous series, the aromatic scaffold next to the carbonyl group presented two different binding locations depending on the compound, while the carbonyl, piperazine and next phenyl ring showed very similar binding for all ligands (**Figure 13B**). In **Figure 13A**, the ligand piperazine and carbonyl groups bound in a polar cavity formed by residues Tyr36, His32 and His167 of one chain, and residues Glu166, Arg177 and Tyr169 of the other chain. In general, the positively charged nitrogen formed a hydrogen bond with Glu166 (See **Figure 13**), which was assisted by interactions with His167, and the carbonyl group bound close to Asn175. Therefore, the presence of a hydrogen bond with Glu166 seems to be of great importance for binding to this enzyme. According to our docking results, the increased length of the linker between the piperazine and the phenyl group resulted in steric hindrance, which did not allow proper binding of the two groups and led to a corresponding decrease in activity (**Supplementary Figure S98B**). Moreover, large and negatively charged substituents of R_3, such as the nitro group, seemed to increase binding by participating in electrostatic interactions with Lys39. Similarly, compound **10** presented a binding mode that differed from the other compounds, with

no hydrogen bond between the piperazine and the glutamate residue, but instead the formation of a salt bridge between the nitro group and Lys39 (**Supplementary Figure S98C**). Finally, substituents in R_1 and R_2 positions may interact with Gln72. However, di-substitution of that phenyl group with large moieties could be responsible for the second binding mode observed for that group in some compounds, and it may be deleterious for affinity.

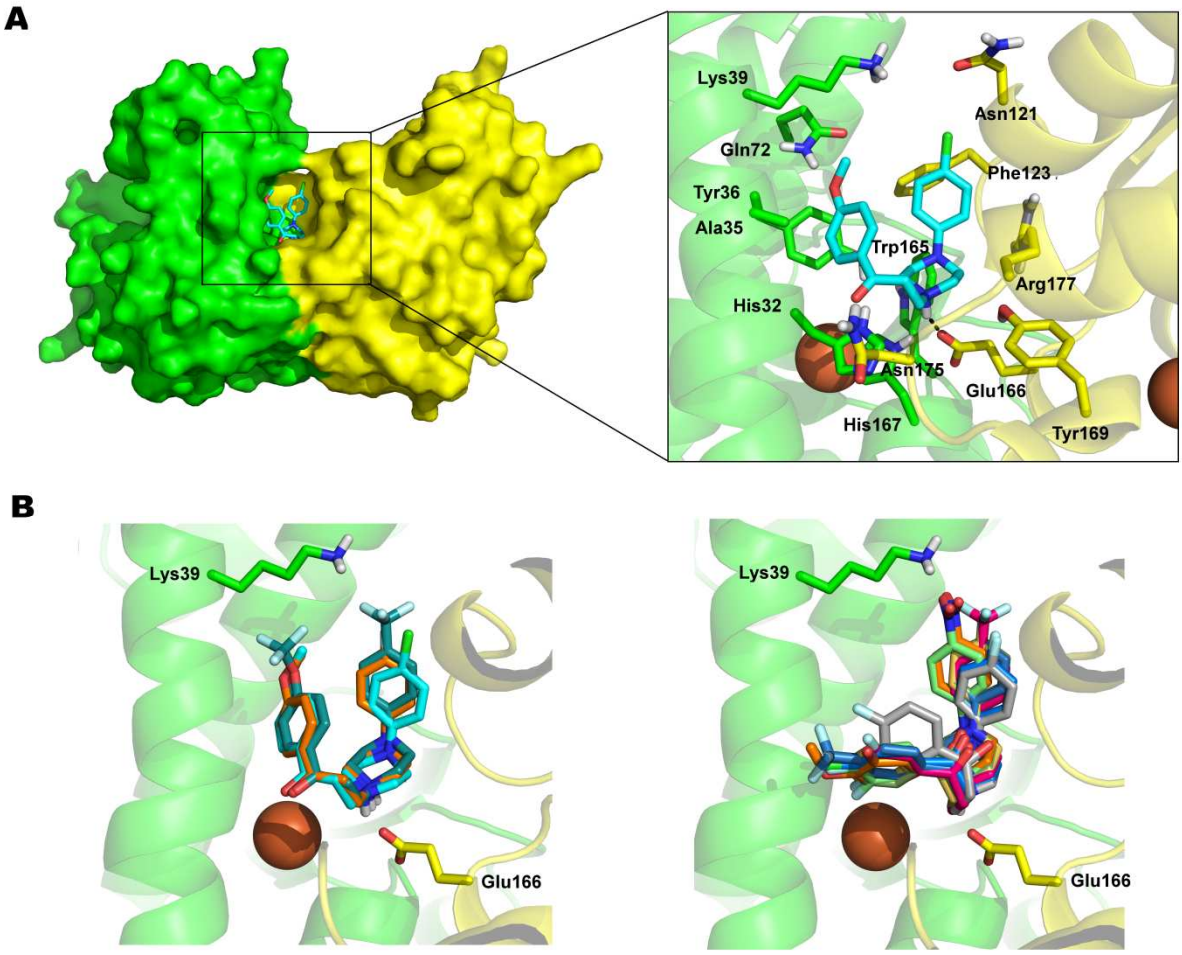

Figure 13. Results of the docking study of the new compounds. **(A)** Proposed binding mode for compound **9** on the Fe-SOD enzyme (PDB entry 4DVH). On the left, the compound is shown binding at the dimer interface, with one protein protomer in green and the other in yellow. In the look-up, the ligand and the residues forming the inhibitor-binding site are shown, colored according to: oxygen

(red), nitrogen (blue), sulfur (yellow), carbon (cyan for compound **10**, and green or yellow for each protein protomer). The iron ions are depicted as brown spheres. **(B)** Two main binding poses obtained. In the left, compounds **7**, **9** and **47**. In the right, compounds **1**, **3**, **8**, **14**, **26**, **31**, **33** and **38.** Same coloring scheme as (**A**) for the protein. Figures were created with The PyMOL Molecular Graphics System, Version 1.8 Schrödinger, LLC.

CONCLUSIONS

In summary, the trypanocidal properties of the second generation of Mannich base-type derivatives were examined both *in vitro* and *in vivo*. The experiments allowed us to select compounds that displayed improved efficiency and lower toxicity than the reference drug BZN. Compounds **7**, **9** and **10** exhibited good *in vitro* trypanocidal properties and a larger spectrum of action, in addition to non-genotoxic capacity. Therefore, they were selected for *in vivo* studies. Compound **10** showed a similar profile to that of BZN in terms of its antiparasitic activity in both the acute and chronic phases, but it was much more promising in relation to its toxicity. Moreover, compound **9** presented a promise *in vivo* trypanocidal activity during both the acute and chronic phases, as well as lower toxicity, lower parasitaemia and fewer organ infections than the reference drug BZN. Parallel studies were carried out to establish the mechanisms of action, which showed that these compounds were selective inhibitors of the Fe-SOD enzyme of *T. cruzi* that cause redox stress due to mitochondrial malfunction, which could be one mechanism underlying their trypanocidal activity. To improve the effectiveness of compound **9**, we must take into consideration further high-level studies, an increase in dosage in future experiments or combined therapies. Moreover, modification of the treatment schedule to achieve better exposure to the compound in the bloodstream should be considered.

Consequently, these Mannich base-type derivatives are promising, simple and appropriately cost-effective candidates for the development of new anti-Chagas agents that could be further assessed in preclinical phase studies.

EXPERIMENTAL SECTION

CHEMISTRY

General methods.

The chemical reagents used for the synthesis were acquired from Panreac Química, Sigma-Aldrich Química, Acros Organics and Alfa Aesar companies. Thin layer chromatography (TLC) was carried out on silica gel 0.2 mm layer (Alugram SIL G/UV254). Synthesis of new compounds was detected at 254 and 360 nm. Flash chromatography was performed on a CombiFlash®RF (Teledyne Isco, Lincoln, USA) instrument with Silica RediSep® columns using a phase normal gradient. The chemical characterization of new compounds was done by infrared (IR) spectra, ^{1}H NMR, carbon nuclear magnetic resonance (^{13}C NMR) and elemental microanalyses (CHN). IR spectra were performed on a Nicolet Nexus FTIR (Thermo Madison, EEUU) using KBr pellets. IR absorption pics signals (cm^{-1}) were expressed as strong (s), medium (m) and weak (w). NMR spectrum of the new compounds dissolved in dimethyl sulfoxide-d_6 (DMSO-d_6) or $CDCl_3$ were determined on a Bruker 400 Ultrashield using tetramethylsilane (TMS) as reference on δ scale. NMR spectra exhibit chemical shifts (parts per million, ppm), coupling constant (*J*) expressed in Hertz (Hz) and the obtained multiplicity were described as singlet (s), bs (broad singlet), doublet (d), doublet of doublets (dd), doublet of doublet doublets (ddd), triplet (t), quadruplet (q) and multiplet (m). In some cases, 2D NMR assays were carried out to get peaks assignment (COSY, HMBC and HMQC). The purity of the new compounds was ≥ 96 % and it was performed on a CHN-900 elemental analyzer (Leco, TresCantos, Spain). The elemental analysis of C, H, N of the previously vacuum-dried compounds were within ±0.4 respect to theoretical value. Melting point was carried out with a Mettler FP82 + FP80 (Greifensee, Switzerland).

Synthesis

Compound **1** was previously reported [40].

The synthesis of compounds **2-17** and **22-49** was carried out by the Mannich reaction following the procedure previously reported by Moreno-Viguri et al. [21]

General method: procedure for the synthesis of compounds 18-21 by nucleophilic substitution: The corresponding alkyl halide (10 mmol), the appropriate piperazine (15 mmol) and K_2CO_3 (10 mmol) were dissolved in 40 mL of THF and maintained with stirring at room temperature for 72 h. Product formation was checked by TLC. The product was extracted with DCM. The organic extract was washed with water, filtered off, dried with anhydrous Na_2SO_4 and evaporated under reduced pressure. The obtained product was purified by precipitation with diethyl ether or by Flash chromatography.

BIOLOGY

Parasite strain culture

Three different *T. cruzi* strains were evaluated: *T. cruzi* SN3 strain (IRHOD/CO/2008/SN3, DTU I) isolated from domestic *Rhodnius prolixus* from Guajira, Colombia [73]; *T. cruzi* Arequipa strain (MHOM/Pe/2011/ Arequipa, DTU V) isolated from a human from Arequipa, Peru; *T. cruzi* Tulahuen strain (TINF/CH/1956/Tulahuen, DTU VI) isolated from Tulahuen, Chile.

Epimastigote culture forms were grown at 28 ºC in RPMI (Gibco®) with 10 % (v/v) heat-inactivated foetal bovine serum (FBS), 0.5 % (w/v) trypticase (BBL) and 0.03 M hemin [74].

***In vitro* activity assays: epimastigote forms (extracellular forms)**

T. cruzi epimastigotes (strains SN3, Arequipa and Tulahuen) were collected in the exponential growth phase by centrifugation at 400 g for 10 min. Assayed compounds and the reference drug BZN were dissolved in DMSO at a concentration of 0.01 % (v/v) to test for nontoxic or inhibitory effects on parasite growth. Trypanocidal activity was determined in our laboratory using the method described by Rolón et al. [75] with some modifications. Assays were performed in 96-well microtiter plates by seeding the parasites at 5×10^5 mL^{-1} after adding the compounds and BZN at dosages of 100 to 0.2 µM and

cultured in 200 µL/well volumes at 28 ºC. Growth controls were also included. After 48 h of incubation, 20 µL of Resazurin sodium salt (0.125 $mg \cdot mL^{-1}$) (Sigma-Aldrich) was added, and the plates were incubated for another 24 h. Finally, 5 µL (10 % w/v) of sodium dodecyl sulphate (SDS) was added, and 10 min later, the trypanocidal activity of the compounds was assessed by absorbance measurements (Sunrise, TECAN) at 570 and 600 nm [76]. The trypanocidal effect was determined using GraphPad Prism and is expressed as the IC_{50}, i.e., the concentration required to result in 50 % inhibition. Each drug concentration was tested in triplicate in four separate determinations.

Cell culture and cytotoxicity tests on Vero cells

Vero cells (EACC number 84113001) from monkey kidney were grown in humidified 95 % air, 5 % CO_2 atmosphere at 37 ºC in RPMI (Gibco®) with 10 % (v/v) heat-inactivated FBS [77].

Vero cells were collected first by trypsinization and then by centrifugation at 400 g for 10 min. The compounds to be tested and the reference drug (BZN) were dissolved as mentioned above.

Cytotoxicity against Vero cells was assessed using 96-well microtiter plates by seeding the cells at 1.25×10^4 mL^{-1} after addition of the compounds and BZN at dosages of 1000 to 1 µM and cultured in 200 µL/well volumes. Growth controls were also included. After 48 h of incubation, the same process as described to determine the trypanocidal activity in the epimastigote forms was followed.

***In vitro* activity assays: amastigote forms (intracellular forms) - infected cells.**

Assays were performed in 24-well microtiter plates by seeding the Vero cells at 1×10^4 $well^{-1}$ with rounded coverslips on the bottom. After 24 h, the cells were infected with culture-derived trypomastigotes of *T. cruzi* (strains SN3, Arequipa and Tulahuen) at a multiplicity of infection (MOI) ratio of 1:10 during 24 h. Non-phagocyted parasites were removed by washing, and after addition of the compounds and BZN at dosages of 100 to 0.2 µM, cultured in 500 µL/well volumes in a humidified 95 % air, 5 % CO_2 atmosphere at 37 ºC. Growth controls were also included. The compounds to be tested and BZN were dissolved as described above. After 72 h of incubation, the trypanocidal effect

was assessed based on the number of amastigotes and infected cells in treated and untreated cultures in methanol-fixed and Giemsa-stained preparations. The number of amastigotes and infected cells was established by analysing 500 host cells distributed in randomly chosen microscopic fields. The infectivity index was defined as the average number of amastigote forms in infected cells multiplied by the percentage of infected cells. The trypanocidal effect was determined using GraphPad Prism and is expressed as the IC_{50}, i.e., the concentration required to result in 50 % inhibition. Each drug concentration was tested in triplicate in four separate determinations.

Transformation of epimastigotes to metacyclic forms.

T. cruzi strains SN3, Arequipa and Tulahuen were grown as epimastigote forms at 28 ºC [78]. Metacyclic trypomastigotes (aged epimastigote cultures) were induced by culturing a 7-day-old culture of epimastigotes in Grace's Insect Medium (Gibco®) with 10 % (v/v) FBS (heat-inactivated) at 28 ºC for 7 days [79]. The parasites were then harvested by centrifugation at 400 g for 10 min and incubated at a density of 5×10^8 mL^{-1} in TAU medium (190 mM NaCl, 17 mM KCl, 2 mM $MgCl_2$, 2 mM $CaCl_2$, 8 mM phosphate buffer, pH 6.0) for 2 h at 28 ºC. Thereafter, the parasites were incubated at a density of 5×10^6 mL^{-1} in TAU3AAG medium (TAU supplemented with 10 mM L-proline, 50 mM L-sodium glutamate, 2 mM L-sodium aspartate and 10 mM D-glucose) for 4 days at 28 ºC [80]. Subsequently, those metacyclic trypomastigotes were used to infect Vero cells in humidified 95 % air, 5 % CO_2 atmosphere at 37 ºC in RPMI (Gibco®) with 10 % (v/v) FBS (heat-inactivated) for 5 to 7 days [81]. Finally, the culture-derived trypomastigotes were collected by centrifugation at 3000 g for 5 min and used to infect BALB/c albino mice.

***In vitro* activity assays: trypomastigote forms (extracellular forms)**

T. cruzi blood trypomastigotes (strain SN3, Arequipa and Tulahuen) were obtain by cardiac puncture from BALB/c albino mice during the parasitaemia peak after infection and diluted in RPMI (Gibco®) with 10 % (v/v) FBS (heat-inactivated). Trypanocidal activity was determined in our

laboratory according to the method described by Faundez et al. [82] with certain modifications. Assays were performed in 96-well microtiter plates by seeding the parasites at 2×10^6 mL^{-1}, and after addition of the compounds and BZN at dosages of 50 to 0.2 μM, cultured in 200 μL/well volumes in a humidified 95 % air, 5 % CO_2 atmosphere at 37 ºC. Growth controls were also included. The compounds to be tested and BZN were dissolved as described above. After 24 h of incubation, 20 μL of Resazurin sodium salt (0.125 $mg \cdot mL^{-1}$) (Sigma-Aldrich) was added, and the plates were incubated for 4 h. Subsequently, the same process as described to determine the trypanocidal activity in epimastigote forms was followed.

***In vitro* genotoxicity screening- SOS/umu assay.**

Bacteria: Salmonella typhimurium TA1535/pSK1002 was purchased from the German Collection for Microorganisms and Cell cultures (DSMZ). *Chemicals:* ampicillin, DMSO, dextrose, KCl, β-mercaptoethanol, $MgSO_4.7H_2O$, NaCl, Na_2CO_3, $Na_2HPO_4.2H_2O$, $NaH_2PO_4.H_2O$, *o*-nitrophenol-β-D-galactopyranoside (ONPG), and SDS were purchased from Sigma-Aldrich. *Biological materials:* Bactotryptone was purchased from BD, and the external metabolic activation system (rat S9 mix) Mutazyme™ was purchased from Moltox. The SOS/umu test was carried out as previously reported by Moreno-Viguri et al. [21]

The assay is considered valid if the positive controls reached an induction factor (IF) ≥ 2 under the established assay conditions. Concentrations at which compounds precipitate are not considered for the corresponding calculations. Thus, a compound was regarded genotoxic if it exhibited an IF ≥ 2 at the non-cytotoxic concentration with a bacterial survival percentage ≥ 80 % under any of the evaluated conditions (with or without metabolic activation), showing a dose-response relationship.

***In vivo* trypanocidal activity assays**

Mice

These experiments were approved by the University of Granada Ethics Committee on Animal Experimentation (RD53/2013) and performed under the rules and principles of the international guide for biomedical research in experimental animals.

Female BALB/c mice (8-10 weeks old and 20-25 g) were used to perform these experiments, maintained under standard conditions (12 h dark/light cycle and 22 ± 3 °C temperature) and provided with water and standard chow *ad libitum*.

Mouse infection and treatment

Groups of six mice were infected via intraperitoneal (i.p.) inoculation with 5 x 10^5 bloodstream trypomastigotes (BTs) of *T. cruzi* Arequipa strain (obtained from previously infected mice with metacyclic trypomastigotes) in 0.2 mL phosphate buffered saline (PBS).

The mice were divided, in the acute and the chronic phase, as follows: 0, negative control group (uninfected and untreated); I, positive control group (infected and untreated); II, BZN group (infected and treated with BZN); III, study group (infected and treated with the compounds under study).

BZN and the compounds under study were prepared at 2 $mg \cdot mL^{-1}$ in an aqueous suspension vehicle containing 5 % (v/v) DMSO and 0.5 % (w/v) hydroxypropyl methylcellulose [83].

Drugs were administered by the oral route (~200 µL) in the treated groups once daily for 5 consecutive days, and vehicle was orally administered in the negative and positive control groups. Therefore, doses of 20 $mg \cdot kg^{-1}$ per day were administered for 5 consecutive days. Administration of the tested compounds was initiated on day 10 post-infection (pi) (once the infection was confirmed) in mice treated in the acute phase and on day 75 pi (once it was established that the animals had entered the chronic phase of the experiment) in the mice treated in the chronic phase.

Parasitaemia levels during treatment in the acute phase

Peripheral blood from each mouse treated in the acute phase was obtained from the mandibular vein (5 µL samples) and diluted 1:100 in PBS. The number of BTs (parasitaemia levels) was quantified

every 2 or 3 days from day 7 pi until the day parasitaemia was not detected. This counting was performed using a Neubauer chamber, and the number of BTs was expressed as parasites·mL^{-1} [84].

Cyclophosphamide-induced IS

After day 100 pi, the groups of mice treated in the acute and chronic phases with significantly decreased parasitaemia levels and established to be in the chronic phase of the experiment, regardless of the treatment and undetectable by fresh blood microscopy examination, were immunosuppressed with CP (ISOPAC®) by i.p. injection with a dose of 200 mg·kg^{-1} every 4 days for a maximum of three doses [83]. The efficacy of such an IS procedure for assessing cryptic infection was verified by the high parasitaemia in chronically untreated mice.

Within 1 week after the last CP injection, parasitaemia was evaluated according the procedure described for parasitaemia levels in the acute phase to quantify the presence or absence of BTs as the reactivation rate.

Organs DNA extraction, PCR and electrophoresis

After cyclophosphamide-induced IS, mice were bled out under gaseous anaesthesia (CO_2) via heart puncture, and blood was collected.

Our previous *in vivo* studies using the *T. cruzi* Arequipa strain revealed its tropism for the following organs: adipose tissue, bone marrow, brain, oesophagus, heart, lung, muscle, spleen and stomach. Therefore, these 9 organs were harvested and immediately perfused with pre-warmed PBS to avoid contamination of the tissue with BTs [85]. In addition, spleen was weighed to evaluate inflammation of this organ in the different groups of mice. Finally, the target organs were thawed and ground up using a Potter-Elvehjem, and DNA was extracted using the Wizard® Genomic DNA Purification Kit (Promega) [84].

PCR was performed based on the published sequence of the enzyme SOD *T. cruzi* CL Brenner (GenBank accession No. XM_808937) using two primers designed in our laboratory (unpublished

data) that allow the detection of *T. cruzi* DNA in different biological samples. These primers amplify a fragment belonging to SOD gene b of *T. cruzi* consisting of approximately 300 base pairs (bp). The amplifications were performed using a Thermal Cycler TM MyCycler thermal cycler (Bio-Rad) with the following reaction mixture: 5 % DMSO, 200 nM iSODd, 200 nM iSODr, 10 mM Tris-HCl (pH 9.0), 1.5 mM $MgCl_2$, 50 mM KCl, 0.01 % gelatine, 0.1 % Triton X-100, 100 mM of each dNTP, 0.5 U of Taq DNA polymerase, 0.05 $\mu g \cdot \mu L^{-1}$ of DNA, and HPLC water, in a final volume of 20 µL; and with the following routine: 95 °C/3 min, 30 cycles of 95 °C/30 s, 55.5 °C/45 s, 72 °C/30 s, and 72 °C/7 min.

Finally, the amplification products were subjected to electrophoresis on a 2 % agarose gel for 90 min at 90 V, containing 1:10000 GelRed nucleic acid gel stain.

ELISA tests

Serum samples were obtained 2 days after treatment, 1 day before IS and on the day of necropsy (sera post-IS) for the mice treated in the acute phase, and 2 days after treatment and on the day of necropsy (sera post-IS) for the mice treated in the chronic phase.

To obtain serum, blood was incubated in a glass tube for 2 h at 37 ºC to allow clotting and then 16 h at 4 ºC for retraction of the clot. The serum was collected and centrifuged at 2700 g for 20 min at 4 ºC. The serum was used for ELISA and biochemical analysis as explained later in this paper. SODe from the parasites, extracted and purified as subsequently described, was used as the antigen fraction.

Circulating antibodies in serum against *T. cruzi* Arequipa strain were qualitatively and quantitatively evaluated by ELISA. The serum from whole blood was diluted 1:80 in PBS, and all serum samples were analysed in triplicate in polystyrene 96-well microtiter plates. The absorbance was read at 492 nm using a microplate reader (Sunrise, TECAN). Mean and standard deviations of the optical densities of the negative control sera were used to calculate the cut-off value (mean plus three times the standard deviation) [84].

Toxicity tests by biochemical analysis

Serum samples were obtained at 2 days after treatment and on the day of necropsy (sera post-IS) both for mice treated in the acute phase and in the chronic phase.

These sera were sent to the Biochemical service in the University of Granada, where a series of parameters were measured using commercial kits from Cromakit® with the BS-200 Chemistry Analyzer Shenzhen Mindray (Bio-medical Electronics Co., LTD).

Mean values and standard deviations were calculated using the levels obtained for different populations of sera (n = 15, n = 6), and the confidence interval for the mean normal populations were also calculated based on a confidence level of 95 % (100 × (1-α) = 100 x (1-0.05)).

Figure 14 shows the timeline for all *in vivo* experiments in the acute and chronic phases.

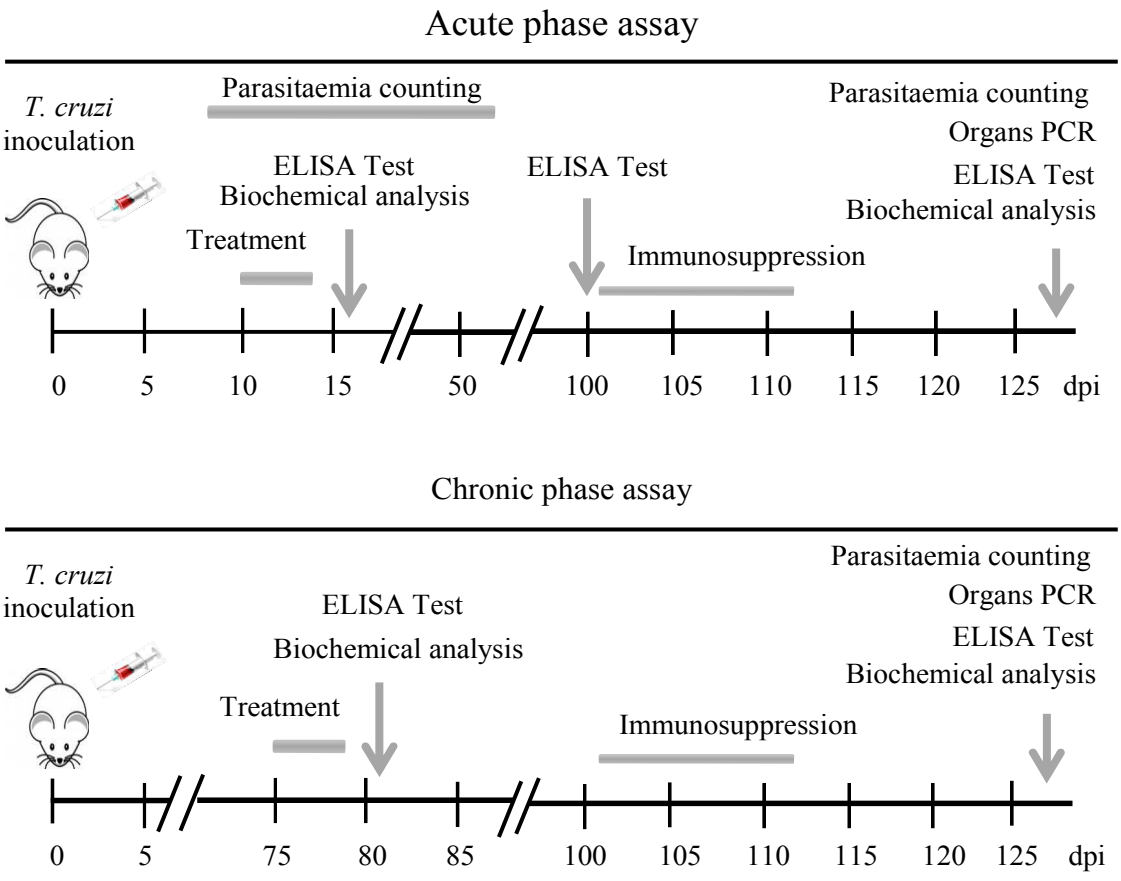

Figure 14. Timeline of *in vivo* experiments in the acute and chronic phases. dpi = day post-infection

Studies of the mechanism of action

Metabolite excretion

T. cruzi strain Arequipa was grown and collected in the epimastigote form at 28 ºC [78] in the exponential growth phase by centrifugation at 400 g for 10 min. The compounds to be tested and the reference drug (BZN) were dissolved as described above. The assays were performed in cell culture flasks (surface area, 25 cm^2) by seeding the parasites at 5×10^5 mL^{-1} and after the addition of the compounds at IC_{25} concentrations at 28 ºC. Non-treated parasites were also included. After 72 h of incubation, treated and non-treated parasites were centrifuged at 800 g for 10 min to collect the supernatants to determine the excreted metabolites by ^1H NMR.

Chemical shifts were expressed in ppm using sodium 2,2-dimethyl-2-silapentane-5-sulphonate as the reference signal. The ^1H NMR spectra were acquired with a VARIAN DIRECT DRIVE 400 MHz Bruker spectrometer with an AutoX probe using D_2O. The chemical shifts used to identify the respective metabolites were consistent with those described previously by our group [86] and with the human metabolome database (http://www.hmdb.ca). The spectral region of 1.0-5.5 ppm was bucketed into a frequency window of 0.1 ppm. The peak (2.6 ppm) corresponding to DMSO was removed before binning, and the regions corresponding to water (4.5-5.5 ppm) and glucose (3.4-3.8 ppm) were excluded during binning to avoid artefacts due to pre-saturation. The aromatic region was excluded because the signal to noise ratio in this region was poorer in comparison to the aliphatic region. The resulting integrals were normalised to the working region (1.0-3.4) ppm of the spectrum to correct for inter-sample differences in dilution. The binning and normalisations were achieved using Mestrenova 9.0 software. The matrix obtained in Mestrenova was imported into Microsoft Excel for further data analyses.

Rho 123 and AO assays.

T. cruzi strain Arequipa was grown, collected and treated as described above (metabolite excretion). Non-treated parasites were also included. After 72 h of incubation, treated and non-treated parasites were collected by centrifugation at 400 g for 10 min, and the pellets of parasites were washed 3 times with PBS. Subsequently, the parasites were resuspended in 0.5 mL PBS with 10 $mg \cdot mL^{-1}$ Rho 123 (Sigma-Aldrich) or 10 $mg \cdot mL^{-1}$ AO (Sigma-Aldrich) for 20 min [87]. Finally, the samples were washed twice with ice-cold PBS, dispersed in 1 mL of PBS and immediately analysed by flow cytometry (BECTON DICKINSON FACSAria III). The data were captured and analysed using BD FACSDiva v8.01 software (Becton Dickinson Biosciences, 2350 Qume Drive, San Jose, Palo-Alto, California). The fluorescence intensities for Rho 123 (mitochondrial membrane potential) and AO (DNA and RNA) were quantified based on the forward (FSC) and side (SSC) scatter, for which a total of 10,000 events were acquired in the previously established region corresponding to *T. cruzi* epimastigotes [88]. Alterations in the fluorescence intensities of AO (APC-A) or Rho 123 (FITC-A) were quantified by the index of variation (IV) obtained using the equation (TM–CM)/CM, where TM is the median fluorescence for treated parasites and CM is the median fluorescence for non-treated parasites (control) [87].

Extraction/purification of the SOD excreted and SOD inhibition studies

T. cruzi strain Arequipa was grown as the epimastigote form at 28 ºC in RPMI (Gibco®) with 10 % (v/v) FBS (heat-inactivated), 0.5 % (w/v) trypticase (BBL) and 0.03 M hemin [74] in the exponential growth phase. The parasites were collected by centrifugation at 400 g for 10 min, and the pellet was resuspended at 5×10^9 mL^{-1} in the same medium without FBS in cell culture flasks (surface area, 75 cm^2). After 28 h of incubation at 28 ºC, the culture was centrifuged at 800 g for 10 min at 4 ºC, and the supernatant was collected and filtered with 0.45-µm pore size filters. Protein was precipitated by addition of ammonium sulphate and centrifugation at 10.000 g for 20 min at 4ºC to maintain the 35-85 % protein fraction, which was redissolved in 2.5 mL of 20 mM potassium phosphate buffer (pH 7.8)

containing 1 mM ethylenediaminetetraacetic acid (EDTA). Finally, this fraction was desalted by gel filtration using a Sephadex G-25 column [88], and the protein concentration was determined using the Bradford method (Sigma Immunochemical, St. Louis) with bovine serum albumin as a standard [89].

Fe-SODe and CuZn-SOD activities were determined using the method described by Beyer and Fridovich [71].

Docking study.

The protonation state of the compounds at pH 7.4 was estimated using the chemicalize webserver (http://www.chemicalize.org/), and they were subsequently designed with the programme Ghemical [90]. For the mitochondrial *T. cruzi* Fe-SOD protein, the structure with Protein Data Bank (PDB) entry 4DVH was used, with residue numbering according to that of Martinez et.al, i.e., without the mitochondrial signal peptide [91]. The protein protonation state at pH 7.4 was obtained with the programme PDB2PQR [92]. Afterwards, Gasteiger charges for both protein and ligands were added with Autodock [93]. The docking study was performed with the Autodock4.0 programme using the Lamarckian genetic algorithm (LGA) [94], with a grid centred on the binding site, as defined in a previous article by our group [21].

ABBREVIATIONS USED

CD, Chagas Disease; *T. cruzi*, *Trypanosoma cruzi*; WHO, World Health Organization; NFX, nifurtimox; BZN, benznidazole; FDA, Food and Drug Administration; TPP, target product profile; DND*i*, Drugs for Neglected Diseases *initiative*; SI, selectivity index; PCR, polymerase chain reaction; SOD, superoxide dismutase; TRase, trypanothione reductase; NTD, neglected tropical disease; PK, pharmacokinetic properties; PD, pharmacodinamic properties; THF, tetrahydrofuran; PSA, polar surface area; DTU, discrete typing unit; IC_{50}, inhibition concentration 50; IS, immunosuppression; Ig, immunoglobulin; ELISA, enzyme-linked immunosorbent assay; pi, post-infection; CP,

cyclophosphamide monohydrate; DNA, deoxyribonucleic acid; bp, base pair; CK-MB, creatine kinase-muscle/brain; LDH, lactate dehydrogenase; AST/GOT, aspartate aminotransferase; ALT/GPT, alanine aminotransferase; ^{1}H NMR, proton nuclear magnetic resonance; NADH, reduced nicotinamide adenine dinucleotide; ATP, adenosine 5′-triphosphate; RNA, ribonucleic acid; PPP, pentose phosphate pathway; TCA, tricarboxylic acid; ADP, adenosine 5′-diphosphate; Rho 123, rhodamine 123; AO, acridine orange; ROS, reactive oxygen species; TLC, thin layer chromatography; DMSO, dimethyl sulfoxide; IR, infrared; ^{13}C NMR, carbon nuclear magnetic resonance; TMS, tetramethylsilane; FBS, foetal bovine serum; SDS, sodium dodecyl sulphate; MOI, multiplicity of infection; ONPG, *o*-nitrophenol-β-D-galactopyranoside; BTs, bloodstream trypomastigotes; PBS, phosphate buffered saline; FSC, forward scatter; SSC, side scatter; EDTA, ethylenediaminetetraacetic acid; PDB, Protein Data Bank.

FINANCIAL SUPPORT

The research leading to these results has received funding from Obra Social la CAIXA and Fundación Caja Navarra, Fundación Roviralta, PROFAND, Ubesol, ACUNSA and Artai. Former Spanish Ministry of Science and Innovation (MICINN), the Ministry of Economy and Competitiveness (MINECO) (project Consolider Ingenio CSD2010-00065) and the Junta de Andalucia (P11-CTS-07187). R.M-E. is grateful for a FPU Grant (FPU14/01537) from the Ministry of Education of Spain. EMC acknowledges a pre-doctoral fellowship from Junta de Andalucia. MJ is indebted to the University of Navarra for a grant. AA thanks the Ministerio de Economía y Competitividad (‘Ramón y Cajal’ programme, 2013) of the Spanish Government for personal support. R.P. is indebted to the Asociación de Amigos de la Universidad de Navarra for a grant.

CONFLICT OF INTEREST

The authors declare no competing financial interest.

AUTHOR INFORMATION

Corresponding author

*Email: cmaris@ugr.es. Phone: (+34) 958 248 886. Current address: Department of Parasitology, Faculty of Sciences (Mecenas), Severo Ochoa s/n, 18001, Granada, Spain.

*Email: sperez@unav.es. Phone: (+34) 948 425 600. Current address: Department of Organic and Pharmaceutical Chemistry, Faculty of Pharmacy, 31008, Pamplona, Spain.

*Email: msanchem@ugr.es. Phone: (+34) 958 242 369. Current address: Department of Parasitology, Faculty of Sciences (Mecenas), Severo Ochoa s/n, 18001, Granada, Spain.

ASSOCIATED CONTENT

Supporting Information.

S1. Compounds characterization

S2. ^{1}H and ^{13}C NMR spectra of newly synthesized compounds.

S3. Molecular formula strings of compounds.

S4. Reduction in the number of T. cruzi amastigote forms per Vero cell.

S5. Results of the SOS/umu screening test.

S6. Binding poses and scores obtained for the docking study in the *T. cruzi* Fe-SOD enzyme.

REFERENCES

1. Rassi, A., Jr.; Rassi, A.; Marin-Neto, J. A. Chagas disease. *Lancet.* **2010,** *375* (9723), 1388–1402.

2. Coura, J. R.; Borges-Pereira, J. Chagas disease: 100 years after its discovery. A systemic review. *Acta trop.* **2010,** *115* (1-2), 5–13.

3. WHO Chagas disease (American trypanosomiasis). http://www.who.int/chagas/en/ (accessed Jun 08, 2016).

4. Schmunis, G. A. Epidemiology of Chagas disease in non-endemic countries: the role of international migration. *Mem. Inst. Oswaldo Cruz.* **2007,** *102 Suppl 1*, 75–85.

5. Bern, C.; Kjos, S.; Yabsley, M. J.; Montgomery, S. P. *Trypanosoma cruzi* and Chagas' Disease in the United States. *Clin. Microbiol. Rev.* **2011,** *24* (4), 655–681.

6. WHO Weekly epidemiological record. http://www.who.int/wer/2015/wer9006.pdf.

7. Coura, J. R.; Dias, J. C. Epidemiology, control and surveillance of Chagas disease: 100 years after its discovery. *Mem. Inst. Oswaldo Cruz.* **2009,** *104 Suppl 1*, 31–40.

8. Osorio, L.; Rios, I.; Gutierrez, B.; Gonzalez, J. Virulence factors of *Trypanosoma cruzi*: who is who? *Microbes. Infect.* **2012,** *14* (15), 1390–1402.

9. Teixeira, A. R.; Nascimento, R. J.; Sturm, N. R. Evolution and pathology in chagas disease--a review. *Mem. Inst. Oswaldo Cruz.* **2006,** *101* (5), 463–491.

10. Messenger, L. A.; Miles, M. A.; Bern, C. Between a bug and a hard place: *Trypanosoma cruzi* genetic diversity and the clinical outcomes of Chagas disease. *Expert Rev. Anti Infect. Ther.* **2015,** *13* (8), 995–1029.

11. Teixeira, A. R.; Hecht, M. M.; Guimaro, M. C.; Sousa, A. O.; Nitz, N. Pathogenesis of chagas' disease: parasite persistence and autoimmunity. *Clin. Microbiol. Rev.* **2011,** *24* (3), 592–630.

12. Flavia Nardy, A.; Freire-de-Lima, C. G.; Morrot, A. Immune Evasion Strategies of *Trypanosoma cruzi*. *J. Immunol. Res.* **2015,** *2015*, 178947.

13. Urbina, J. A. Specific chemotherapy of Chagas disease: relevance, current limitations and new approaches. *Acta trop.* **2010,** *115* (1-2), 55–68.

14. Rodriques Coura, J.; de Castro, S. L. A critical review on Chagas disease chemotherapy. *Mem. Inst. Oswaldo Cruz.* **2002,** *97* (1), 3–24.

15. (a) FDA Food and Drug Administration, 2018. https://www.accessdata.fda.gov/drugsatfda_docs/label/2017/209570lbl.pdf/

(b) FDA Food and Drug Administration, 2018. https://newdrugapprovals.org/2017/08/30/fda-approves-first-u-s-treatment-benznidazole-for-chagas-disease/ (accessed Feb 20, 2018).

16. Chatelain, E. Chagas disease drug discovery: toward a new era. *J. Biomol. Screen.* **2015,** *20* (1), 22–35.

17. Molina, I.; Salvador, F.; Sanchez-Montalva, A. [Update Chagas disease]. *Enferm. Infecc. Microbiol. Clin.* **2016,** *34* (2), 132–138.

18. Molina, I.; Gomez i Prat, J.; Salvador, F.; Trevino, B.; Sulleiro, E.; Serre, N.; Pou, D.; Roure, S.; Cabezos, J.; Valerio, L.; Blanco-Grau, A.; Sanchez-Montalva, A.; Vidal, X.; Pahissa, A. Randomized trial of posaconazole and benznidazole for chronic Chagas' disease. *N. Engl. J. Med.* **2014,** *370* (20), 1899–1908.

19. Porras, A. I.; Yadon, Z. E.; Altcheh, J.; Britto, C.; Chaves, G. C.; Flevaud, L.; Martins-Filho, O. A.; Ribeiro, I.; Schijman, A. G.; Shikanai-Yasuda, M. A.; Sosa-Estani, S.; Stobbaerts, E.; Zicker, F. Target Product Profile (TPP) for Chagas Disease Point-of-Care Diagnosis and Assessment of Response to Treatment. *PLoS Negl. Trop. Dis.* **2015,** *9* (6), e0003697.

20. Bala, S.; Sharma, N.; Kajal, A.; Kamboj, S.; Saini, V. Mannich bases: an important pharmacophore in present scenario. *Int. J. Med. Chem.* **2014,** *2014*, 191072.

21. Moreno-Viguri, E.; Jimenez-Montes, C.; Martin-Escolano, R.; Santivañez-Veliz, M.; Martin-Montes, A.; Azqueta, A.; Jimenez-Lopez, M.; Zamora Ledesma, S.; Cirauqui, N.; Lopez de Cerain, A.; Marin, C.; Sanchez-Moreno, M.; Perez-Silanes, S. *In Vitro* and *in Vivo* Anti-*Trypanosoma cruzi*

Activity of New Arylamine Mannich Base-Type Derivatives. *J.Med. Chem.* **2016,** *59* (24), 10929-10945.

22. Roman, G. Mannich bases in medicinal chemistry and drug design. *Eur. J. Med. Chem.* **2015,** *89*, 743–816.

23. Koksal, M.; Gokhan, N.; Kupeli, E.; Yesilada, E.; Erdogan, H. Analgesic and antiinflammatory activities of some new Mannich bases of 5-nitro-2-benzoxazolinones. *Arch. Pharm. Res.* **2007,** *30* (4), 419–424.

24. Ivanova, Y.; Momekov, G.; Petrov, O.; Karaivanova, M.; Kalcheva, V. Cytotoxic Mannich bases of 6-(3-aryl-2-propenoyl)-2(3H)-benzoxazolones. *Eur. J. Med. Chem.* **2007,** *42* (11-12), 1382–1387.

25. Gul, H. I.; Vepsalainen, J.; Gul, M.; Erciyas, E.; Hanninen, O. Cytotoxic activities of mono and bis Mannich bases derived from acetophenone against Renca and Jurkat cells. *Pharm. Acta Helv.* **2000,** *74* (4), 393–398.

26. Ashok, M.; Holla, B. S.; Poojary, B. Convenient one pot synthesis and antimicrobial evaluation of some new Mannich bases carrying 4-methylthiobenzyl moiety. *Eur. J. Med. Chem.* **2007,** *42* (8), 1095–1101.

27. Gul, H. I.; Ojanen, T.; Vepsalainen, J.; Gul, M.; Erciyas, E.; Hanninen, O. Antifungal activity of some mono, bis and quaternary Mannich bases derived from acetophenone. *Arzneimittelforschung.* **2001,** *51* (1), 72–75.

28. Sriram, D.; Banerjee, D.; Yogeeswari, P. Efavirenz Mannich bases: synthesis, anti-HIV and antitubercular activities. *J. Enzyme Inhib. Med. Chem.* **2009,** *24* (1), 1–5.

29. Roy, S.; Chetia, D.; Rudrapal, M.; Prakash, A. Synthesis and antimalarial activity study of some new Mannich bases of 7-chloro-4-aminoquinoline. *Med. Chem.* **2013,** *9* (3), 379–383.

30. Wenzel, I. N.; Wong, P. E.; Maes, L.; Muller, T. J.; Krauth-Siegel, R. L.; Barrett, M. P.; Davioud-Charvet, E. Unsaturated Mannich bases active against multidrug-resistant *Trypanosoma brucei brucei* strains. *Chem. Med. Chem.* **2009,** *4* (3), 339–351.

31. Lee, B.; Bauer, H.; Melchers, J.; Ruppert, T.; Rattray, L.; Yardley, V.; Davioud-Charvet, E.; Krauth-Siegel, R. L. Irreversible inactivation of trypanothione reductase by unsaturated Mannich bases: a divinyl ketone as key intermediate. *J.Med. Chem.* **2005,** *48* (23), 7400-7410.

32. Papadopoulou, M. V.; Bloomer, W. D.; Rosenzweig, H. S.; O'Shea, I. P.; Wilkinson, S. R.; Kaiser, M. 3-Nitrotriazole-based piperazides as potent antitrypanosomal agents. *Eur J Med Chem.* **2015,** *103*, 325–334.

33. Papadopoulou, M. V.; Trunz, B. B.; Bloomer, W. D.; McKenzie, C.; Wilkinson, S. R.; Prasittichai, C.; Brun, R.; Kaiser, M.; Torreele, E. Novel 3-Nitro-1H-1,2,4-triazole-Based Aliphatic and Aromatic Amines as Anti-Chagasic Agents. *J.Med. Chem.* **2011,** *54* (23), 8214–8223.

34. Papadopoulou, M. V.; Bloomer, W. D.; Rosenzweig, H. S.; Kaiser, M.; Chatelain, E.; Ioset, J. R. Novel 3-nitro-1H-1,2,4-triazole-based piperazines and 2-amino-1,3-benzothiazoles as antichagasic agents. *Bioorg. Chem.* **2013,** *21* (21), 6600–6607.

35. Corona, P.; Gibellini, F.; Cavalli, A.; Saxena, P.; Carta, A.; Loriga, M.; Luciani, R.; Paglietti, G.; Guerrieri, D.; Nerini, E.; Gupta, S.; Hannaert, V.; Michels, P. A. M.; Ferrari, S.; Costi, P. M. Structure-Based Selectivity Optimization of Piperidine-Pteridine Derivatives as Potent Leishmania Pteridine Reductase Inhibitors. *J.Med. Chem.* **2012,** *55* (19), 8318–8329.

36. Saenz, R. E.; Paz, H.; Berman, J. D. Efficacy of ketoconazole against Leishmania braziliensis panamensis cutaneous leishmaniasis. *Am. J. Med.* **1990,** *89* (2), 147–155.

37. Al-Mutairi, N.; Alshiltawy, M.; El Khalawany, M.; Joshi, A.; Eassa, B. I.; Manchanda, Y.; Gomaa, S.; Darwish, I.; Rijhwani, M. Tropical medicine rounds: Treatment of Old World cutaneous

leishmaniasis with dapsone, itraconazole, cryotherapy, and imiquimod, alone and in combination. *Int. J. Dermatol.* **2009,** *48* (8), 862–869.

38. El-Sayed, M.; Anwar, A. E. Intralesional sodium stibogluconate alone or its combination with either intramuscular sodium stibogluconate or oral ketoconazole in the treatment of localized cutaneous leishmaniasis: a comparative study. *J. Eur. Acad. Dermatol. Venereol.* **2010,** *24* (3), 335–340.

39. Urbina, J. A. Ergosterol biosynthesis and drug development for Chagas disease. *Mem. Inst. Oswaldo Cruz*. **2009,** *104*, 311–318.

40. Martinez-Esparza, J.; Oficialdegui, A. M.; Perez-Silanes, S.; Heras, B.; Orus, L.; Palop, J. A.; Lasheras, B.; Roca, J.; Mourelle, M.; Bosch, A.; Del Castillo, J. C.; Tordera, R.; Del Rio, J.; Monge, A. New 1-aryl-3-(4-arylpiperazin-1-yl)propane derivatives, with dual action at 5-HT1A serotonin receptors and serotonin transporter, as a new class of antidepressants. *J.Med. Chem.* **2001,** *44* (3), 418–428.

41. Sander, T.; Freyss, J.; von Korff, M.; Rufener, C. DataWarrior: An Open-Source Program For Chemistry Aware Data Visualization And Analysis. *J. Chem. Inf. Model.* **2015,** *55* (2), 460-473.

42. Zingales, B. *Trypanosoma cruzi* genetic diversity: Something new for something known about Chagas disease manifestations, serodiagnosis and drug sensitivity. *Acta Trop*. **2017**, S0001-706X(17)30426-6.

43. González, P.; Marin, C.; Rodriguez-González, I.; Hitos, A. B.; Rosales, M. J.; Reina, M.; Díaz, J. G.; González-Coloma, A.; Sánchez-Moreno, M. *In vitro* activity of C20-diterpenoid alkaloid derivatives in promastigotes and intracellular amastigotes of *Leishmania infantum*. *Int. J. Antimicrob. Agents*. **2005**, *25* (2), 136–141.

44. Nwaka, S.; Besson, D.; Ramirez, B.; Maes,L.; Matheeussen, A.; Bickle, Q.; Mansour, N. R.; Yousif, F.; Townson, S.; Gokool, S.; Cho-Ngwa, F.; Samje, M.; Misra-Bhattacharya, S.; Murthy, P. K.;

Fakorede, F.; Paris, J. M.; Yeates, C.; Ridley, R.; Van Voorhis, W. C.; Geary, T. Integrated dataset of screening hits against multiple neglected disease pathogens. *PLoS Negl. Trop. Dis*. **2011**, *5* (12), e1412.

45. Fabbro De Suasnábar, D.; Arias, E.; Streiger, M.; Piacenza, M.; Ingaramo, M.; Del Barco, M.; Amicone, N. Evolutive behavior towards cardiomyopathy of treated (nifurtimox or benznidazole) and untreated chronic chagasic patients. *Rev. Inst. Med. Trop. Sao Paulo*. **2000**, *42* (2), 99–109.

46. Espuelas, S.; Plano, D.; Nguewa, P.; Font, M.; Palop, J. A.; Irache, J. M.; Sanmartin, C. Innovative Lead Compounds and Formulation Strategies As Newer Kinetoplastid Therapies. *Curr. Med. Chem*. **2012**, *19* (25), 4259–4288.

47. Urbina, J. A. Chemotherapy of Chagas disease. *Curr. Pharm. Des*. **2002**, *8* (4), 287–295.

48. Santos, D. M.; Martins, T. A.; Caldas, I. S.; Diniz, L. F.; Machado-Coelho, G. L.; Carneiro, C. M.; Oliveira, R. de P.; Talvani, A.; Lana, M.; Bahia, M. T. Benznidazole alters the pattern of Cyclophosphamide-induced reactivation in experimental *Trypanosoma cruzi*-dependent lineage infection. *Acta Trop*. **2010**, *113* (2), 134–138.

49. Murcia, L.; Carrilero, B.; Ferrer, F.; Roig, M.; Franco, F.; Segovia, M. Success of benznidazole chemotherapy in chronic *Trypanosoma cruzi*-infected patients with a sustained negative PCR result. *Eur.J.Clin. Microbiol. Infect*. Dis. **2016**, *35* (11), 1819–1827.

50. Basquiera, A. L.; Sembaj, A.; Aguerri, A. M.; Omelianiuk, M.; Guzmán, S.; Moreno Barral, J.; Caeiro, T. F.; Madoery, R. J.; Salomone, O. A. Risk progression to chronic Chagas cardiomyopathy: influence of male sex and of parasitaemia detected by polymerase chain reaction. *Heart*. **2003**, *89* (10), 1186–1190.

51. Williams, J. T.; Mubiru, J. N.; Schlabritz-Loutsevitch, N. E.; Rubicz, R. C.; VandeBerg, J.L.; Dick, E. J. Jr; Hubbard, G. B. Polymerase chain reaction detection of *Trypanosoma cruzi* in Macaca fascicularis using archived tissues. *Am. J. Trop. Med. Hyg*. **2009**, *81* (2), 228–234.

52. Britto, C.; Cardoso, M.A.; Marques, P.; Fernandes, O.; Morel, C. M. Polymerase chain reaction detection: new insights into the diagnosis of chronic Chagas disease. *Mem. Inst. Oswaldo Cruz*. **1999**, *94* (1), 305–306.

53. Francisco, A. F.; Lewis, M. D.; Jayawardhana, S.; Taylor, M. C.; Chatelain, E.; Kelly, J. M. Limited Ability of Posaconazole To Cure both Acute and Chronic *Trypanosoma cruzi* Infections Revealed by Highly Sensitive *In Vivo* Imaging. *Antimicrob. Agents Chemother*. **2015**, *59* (8), 4653–4661.

54. El Bouhdidi, A.; Truyens, C.; Rivera, M. T.; Bazin, H.; Carlier, Y. *Trypanosoma cruzi* infection in mice induces a polyisotypic hypergammaglobulinaemia and parasite-specific response involving high IgG2a concentrations and highly avid IgG1 antibodies. *Parasite Immunol*. **1994**, 16 (2), 69–76.

55. Kayama, H.; Takeda, K. The innate immune response to *Trypanosoma cruzi* infection. *Microbes Infect*. **2010**, *12* (7), 511–517.

56. Ginger, M. L. Trypanosomatid biology and euglenozoan evolution: new insights and shifting paradigms revealed through genome sequencing. *Protist*. **2005**, *156* (4), 337–392.

57. Bringaud, F.; Rivière, L.; Coustou, V. Energy metabolism of trypanosomatids: adaptation to available carbon sources. *Mol. Biochem. Parasitol*. **2006**, *149* (1), 1–9.

58. Stoppani, A. O.; Docampo, R.; de Boiso, J. F.; Frasch, A. C. Effect of inhibitors of electron transport and oxidative phosphorylation on *Trypanosoma cruzi* respiration and growth. *Mol. Biochem. Parasitol*. **1980**, *2* (1), 3–21.

59. Cazzulo, J. J. Aerobic fermentation of glucose by trypanosomatids. *FASEB J*. **1992**, *6* (13), 3153–3161.

60. Kirkinezos, I. G.; Moraes, C. T. Reactive oxygen species and mitochondrial diseases. *Semin. Cell Dev. Biol*. **2001**, *12* (6), 449–457.

61. Michels, P. A.; Bringaud, F.; Herman, M.; Hannaert, V. Metabolic functions of glycosomes in trypanosomatids. *Biochim. Biophys. Acta*. **2006**, *1763* (12), 1463–1477.

62. Shang, X. J.; Yao, G.; Ge, J. P.; Sun, Y.; Teng, W. H.; Huang, Y. F. Procyanidin induces apoptosis and necrosis of prostate cancer cell line PC-3 in a mitochondrion-dependent manner. *J. Androl.* **2009**, *30* (2), 122–126.

63. Lee, W. K.; Thévenod, F. A role for mitochondrial aquaporins in cellular life-and-death decisions? *Am. J. Physiol. Cell Physiol*. **2006**, *291* (2), 195–202.

64. Wen, J. J.; Gupta, S.; Guan, Z.; Dhiman, M.; Condon, D.; Lui, C.; Garg, N. J. Phenyl-alpha-tert-butyl-nitrone and benzonidazole treatment controlled the mitochondrial oxidative stress and evolution of cardiomyopathy in chronic chagasic Rats. *J. Am. Coll. Cardiol*. **2010**, *55* (22), 2499–2508.

65. Hall, B. S.; Wilkinson, S. R. Activation of Benznidazole by Trypanosomal Type I Nitroreductases Results in Glyoxal Formation. *Antimicrob. Agents Chemother*. **2012**, *56* (1), 115–123.

66. Verma, N. K.; Singh, G.; Dey, C. S. Miltefosine induces apoptosis in arsenite-resistant *Leishmania donovani* promastigotes through mitochondrial dysfunction. *Exp. Parasitol*. **2007**, *166* (1), 1–13.

67. Hunter, W. N.; Alphey, M. S.; Bond, C. S.; Schüttelkopf, A. W. Targeting metabolic pathways in microbial pathogens: oxidative stress and anti-folate drug resistance in trypanosomatids. *Biochem. Soc. Trans*. **2003**, *31* (Pt 3), 607–610.

68. Piacenza, L.; Zago, M. P.; Peluffo, G.; Alvarez, M. N.; Basombrio, M. A.; Radi, R. Enzymes of the antioxidant network as novel determiners of *Trypanosoma cruzi* virulence. *Int. J.Parasitol.* **2009**, *39* (13), 1455–1464.

69. Maes, L.; Vanden Berghe, D.; Germonprez, N.; Quirijnen, L.; Cos, P.; De Kimpe, N.; Van Puyvelde, L. *In vitro* and *in vivo* activities of a triterpenoid saponin extract (PX-6518) from the plant

Maesa balansae against visceral leishmania species. *Antimicrob.Agents Chemother*. **2004**, *48* (1), 130–136.

70. Germonprez, N.; Maes, L.; Van Puyvelde, L.; Van Tri, M.; Tuan, D. A.; De Kimpe, N. *In vitro* and *in vivo* anti-leishmanial activity of triterpenoid saponins isolated from Maesa balansae and some chemical derivatives. *J. Med. Chem*. **2005**, *48* (1), 32–37.

71. Beyer, W. F.; Fridovich, I. Assaying for superoxide dismutase activity: some large consequences of minor changes in conditions. *Anal. Biochem*. **1897**, *161*, 559–566.

72. Docampo, R. Sensitivity of parasites to free radical damage by antiparasitic drugs. *Chem. Biol. Interact*. **1990**, *73* (1), 1–27.

73. Téllez-Meneses, J.; Mejía-Jaramillo, A. M.; Triana-Chávez, O. Biological characterization of *Trypanosoma cruzi* stocks from domestic and sylvatic vectors in Sierra Nevada of Santa Marta, Colombia. *Acta Trop.* **2008**, *108* (1), 26–34.

74. Kendall, G.; Wilderspin, A. F.; Ashall, F.; Miles, M. A.; Kelly, J. M. *Trypanosoma cruzi* glycosomal glyceraldehyde-3-phosphate dehydrogenase does not conform to the "hotspot" topogenic signal model. *EMBO J*. **1990**, *9* (9), 2751–2758.

75. Rolón, M.; Vega, C.; Escario, J. A.; Gómez-Barrio, A. Development of resazurin microtiter assay for drugs sensibility testing of *Trypanosoma cruzi* epimastigotes. *Parasitol. Res*. **2006**, *99* (2), 103–107.

76. Rampersad, S. N. Multiple applications of Alamar Blue as an indicator of metabolic function and cellular health in cell viability bioassays. *Sensors* **2012**, *12* (9), 12347–12360.

77. Pless-Petig, G.; Metzenmacher, M.; Türk, T. R.; Rauen, U. Aggravation of cold-induced injury in Vero-B4 cells by RPMI 1640 medium - identification of the responsible medium components. *BMC Biotechnol*. **2012**, *10*, 12–73.

78. Bahia, M. T.; de Andrade, I. M.; Martins, T. A.; do Nascimento, Á. F.; Diniz, Lde F.; Caldas, I. S.; Talvani, A.; Trunz, B. B.; Torreele, E.; Ribeiro, I. Fexinidazole: a pontential new drug candidate for Chagas Disease. *PloS Negl. Trop. Dis*. **2012**, *6* (11), e1870.

79. Isola, E. L.; Lammel, E. M.; González Cappa, S. M. *Trypanosoma cruzi*: differentiation after interaction of epimastigotes and *Triatoma infestans* intestinal homogenate. *Exp. Parasitol*. **1986**, *62* (3), 329–335.

80. Cardoso, J.; Soares, M. J. *In vitro* effects of citral on *Trypanosoma cruzi* metacyclogenesis. *Mem. Inst. Oswaldo Cruz* **2010**, *105* (8), 1026–1032.

81. Contreras, V. T.; Salles, J. M.; Thomas, N.; Morel, C. M.; Goldenberg, S. *In vitro* differentiation of *Trypanosoma cruzi* under chemically defined conditions. *Mol. Biochem. Parasitol*. **1985**, *16* (3), 315–327.

82. Faundez, M.; Pino, L.; Letelier, P.; Ortiz, C.; López, R.; Seguel, C.; Ferreira, J.; Pavani, M.; Morello, A.; Maya, J. D. Buthionine sulfoximine increases the toxicity of nifurtimox and benznidazole to *Trypanozoma cruzi*. *Amtimicrob. Agents Chemother*. **2005**, *49* (1), 126–130.

83. Francisco, A. F.; Jayawardhana, S.; Lewis, M. D.; White, K. L.; Shackleford, D. M.; Chen, G.; Saunders, J.; Osuna-Cabello, M.; Read, K. D.; Charman, S. A.; Chatelain, E.; Kelly, J. M. Nitroheterocyclic drugs cure experimental *Trypanosoma cruzi* infections more effectively in the chronic stage than in the acute stage. *Sci. Rep*. **2016**, 6: 35351.

84. Olmo, F.; Rotger, C.; Ramírez-Macías, I.; Martínez, L.; Marín, C.; Carreras, L.; Urbanová, K.; Vega, M.; Chaves-Lemaur, G.; Sampedro, A.; Rosales, M. J.; Sánchez-Moreno, M.; Costa, A. Synthesis and biological evaluation of N,N'-squaramides with high *in vivo* efficacy and low toxicity: towards a low-cost drug against Chagas Disease. *J.Med. Chem*. **2014**, *57* (3), 987–999.

85. Ye, X.; Ding, J.; Zhou, X.; Chen, G.; Liu, S. F. Divergent roles of endothelial NF-kappaB in multiple organ injury and bacterial clearance in mouse models of sepsis. *J. Exp. Med.* **2008**, *205* (6), 1303–1315.

86. Fernandez-Becerra, C.; Sanchez-Moreno, M.; Osuna, A.; Opperdoes. F.R. Comparative aspects of energy metabolism in plant trypanosomatids. *J. Euk. Microbiol.* **1997**, *44* (5), 523–529.

87. Sandes, J. M.; Fontes, A.; Regis-da-Silva, C. G.; de Castro, M. C.; Lima-Junior, C. G.; Silva, F. P.; Vasconcellos, M. L.; Figueiredo, R. C. *Trypanosoma cruzi* cell death induced by the Morita-Baylis-Hillman adduct 3-Hydroxy-2-methylene-3-nitrophenylpropanenitrile). *PLoS One* **2014**, *9* (4), e93936.

88. Hussein, N.; Amawi, H.; Karthikeyan, C.; Hall, F. S.; Mittal, R.; Trivedi, P.; Ashby, C. R. Jr; Tiwari, A. K. The dopamine D3 receptor antagonists PG01037, NGB2904, SB277011A, and U99194 reverse ABCG2 transporter-mediated drug resistance in cancer cell lines. *Cancer Lett*. **2017**, *396*, 167–180.

89. Bradford, M. M. A refined and sensitive method for the quantification of microgram quantities of protein utilizing the principle of protein-dye binding. *Anal. Biochem.* **1976**, *72*, 248–254.

90. Hassinen, T.; Perakyla, M. New energy terms for reduced protein models implemented in an off-lattice force field. *J. Comput. Chem*. **2001**, *22*, 1229–1242.

91. Martinez, A.; Peluffo, G.; Petruk, A. A.; Hugo, M.; Piñeyro, D.; Demicheli, V.; Moreno, D. M.; Lima, A.; Batthyány, C.; Durán, R.; Robello, C.; Martí, M.A.; Larrieux, N.; Buschiazzo, A.; Trujillo, M.; Radi, R.; Piacenza, L. Structural and molecular basis of the peroxynitrite-mediated nitration and inactivation of *Trypanosoma cruzi* iron-superoxide dismutases (Fe-SODs) A and B: disparate susceptibilities due to the repair of Tyr35 radical by Cys83 in Fe-SODB through intramolecular electron transfer. *J Biol Chem*. **2014**, *289* (18), 12760–12778.

92. Dolinsky, T. J.; Czodrowski, P.; Li, H.; Nielsen, J. E.; Jensen, J. H.; Klebe, G.; Baker, N. A. PDB2PQR: expanding and upgrading automated preparation of biomolecular structures for molecular simulations. *Nucleic. Acids Research*. **2007**, *35*, W522–W525.

93. Morris, G. M.; Huey, R.; Lindstrom, W.; Sanner, M. F.; Belew, R. K.; Goodsell, D. S.; Olson, A. J. AutoDock4 and AutoDockTools4: Automated docking with selective receptor flexibility. *J. Comput. Chem*. **2009**, *30*, 2785–2791.

94. Huey, R.; Morris, G. M.; Olson, A. J.; Goodsell, D. S. A semiempirical free energy force field with charge-based desolvation. *J. Comput. Chem*. **2007**, *28*, 1145–1152.

TOC.

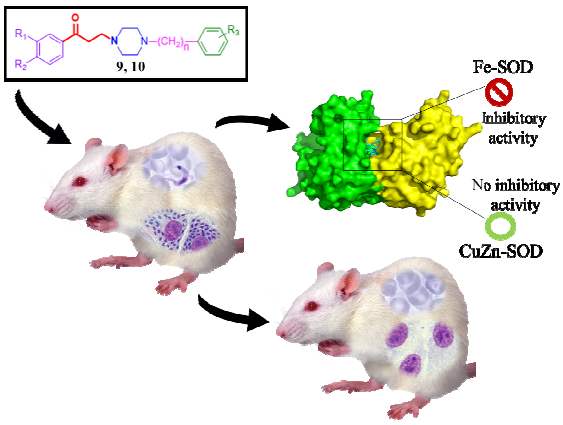
9, 10
Fe-SOD
Inhibitory activity
No inhibitory activity
CuZn-SOD


A
Lys39
Tyr36
Phe123
Asn12
His32
Arg177
Glu166

B
F
S
cyclic
amine
EW

R1
R2
N
N
(CH2)n
R3

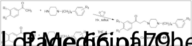

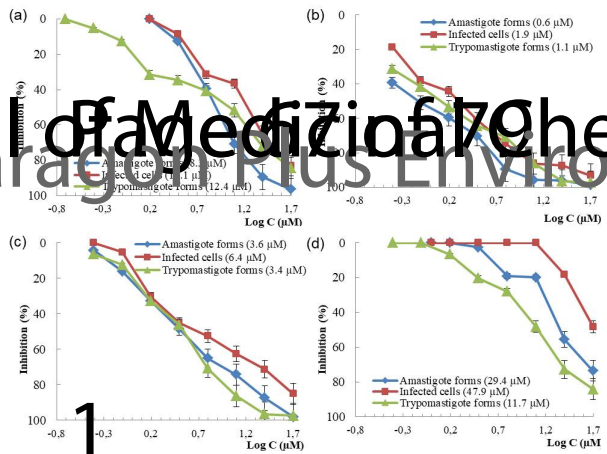
(a)
Inhibition (%)
Log C (μM)
Amastigote forms (8.8 μM)
Infected cells (11 μM)
Trypomastigote forms (12.4 μM)
(b)
Amastigote forms (0.6 μM)
Infected cells (1.9 μM)
Trypomastigote forms (1.1 μM)
Inhibition (%)
Log C (μM)
(c)
Amastigote forms (3.6 μM)
Infected cells (6.4 μM)
Trypomastigote forms (3.4 μM)
Inhibition (%)
Log C (μM)
(d)
Amastigote forms (29.4 μM)
Infected cells (47.9 μM)
Trypomastigote forms (11.7 μM)
Inhibition (%)
Log C (μM)

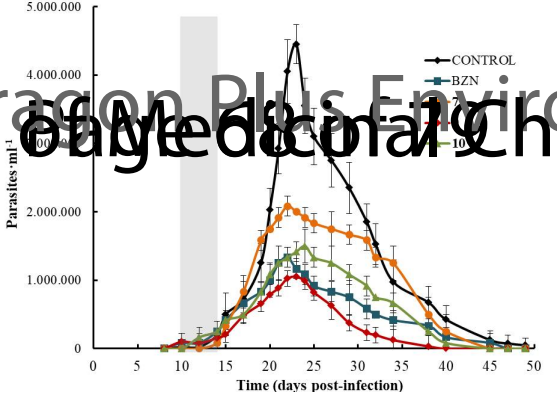
5.000.000
4.000.000
3.000.000
2.000.000
1.000.000
0
Parasites·ml-1
0
5
10
15
20
25
30
35
40
45
50
Time (days post-infection)
CONTROL
BZN
10

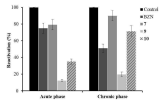

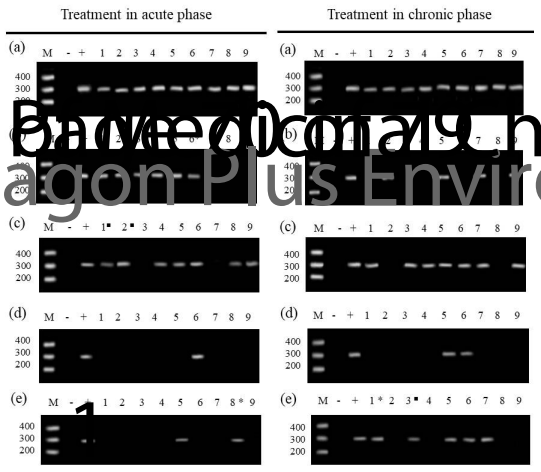
Treatment in acute phase
Treatment in chronic phase
(a)
M - + 1 2 3 4 5 6 7 8 9
400
300
200
(b)
(c)
(d)
(e)

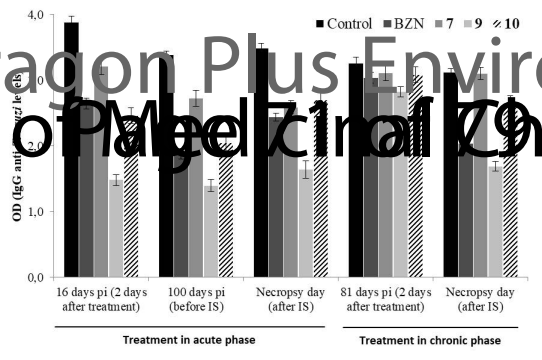
Control
BZN
7
9
10
OD (IgG anti-Toxo level)
4,0
3,0
2,0
1,0
0,0
16 days pi (2 days after treatment)
100 days pi (before IS)
Necropsy day (after IS)
81 days pi (2 days after treatment)
Necropsy day (after IS)
Treatment in acute phase
Treatment in chronic phase

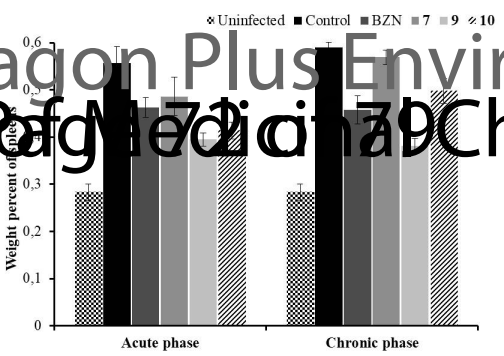
Uninfected
Control
BZN
7
9
10
Weight percent of pleu
0,6
0,5
0,4
0,3
0,2
0,1
0
Acute phase
Chronic phase

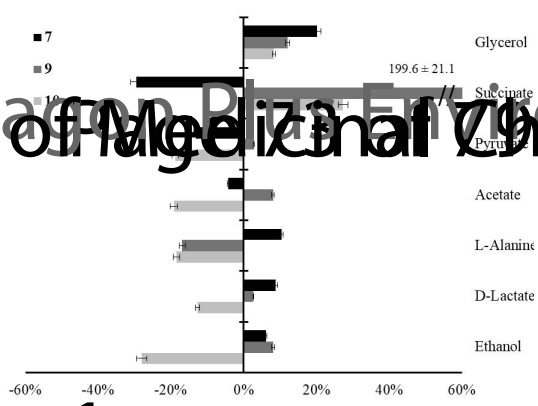
7
9
Glycerol
199.6 ± 21.1
Succinate
Pyruvate
Acetate
L-Alanine
D-Lactate
Ethanol
-60%
-40%
-20%
0%
20%
40%
60%

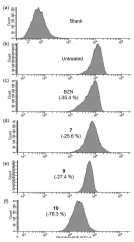
Blank
Untreated
BZN
(-55.4 %)
7
(-23.6 %)
9
(-27.4 %)
10
(-18.3 %)

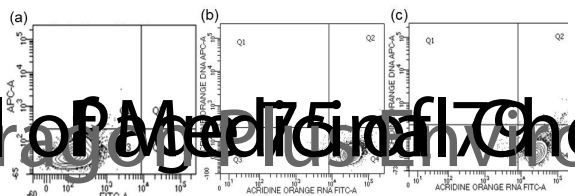

1

Compound	BZN	7	9	10
Inhibition (%)	22.4	24.6	18.0	72.9

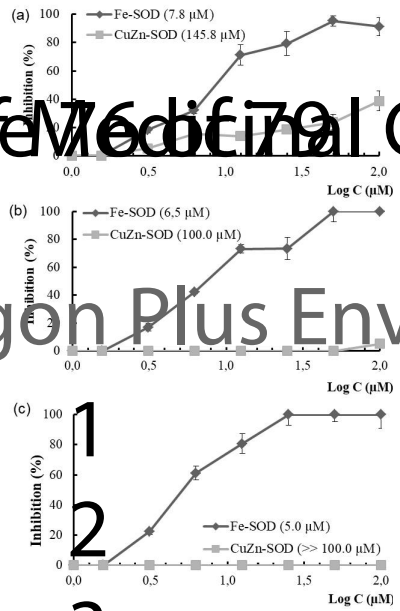
(a)
Fe-SOD (7.8 μM)
CuZn-SOD (145.8 μM)
Inhibition (%)
Log C (μM)
(b)
Fe-SOD (6,5 μM)
CuZn-SOD (100.0 μM)
Inhibition (%)
Log C (μM)
(c)
Inhibition (%)
Fe-SOD (5.0 μM)
CuZn-SOD (>> 100.0 μM)
Log C (μM)

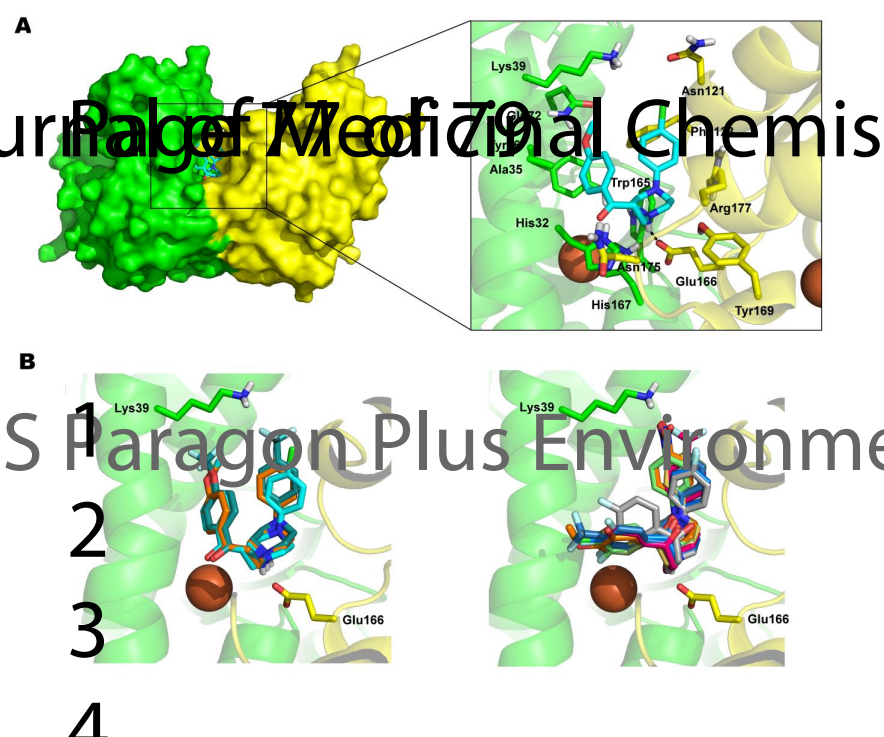
A
Lys39
Asn121
Ala35
Trp165
Arg177
His32
Asn175
Glu166
His167
Tyr169
B
Lys39
Glu166
Lys39
Glu166

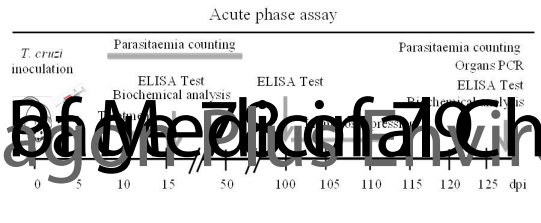
Acute phase assay
T. cruzi inoculation
Parasitaemia counting
ELISA Test
Biochemical analysis
ELISA Test
Parasitaemia counting
Organs PCR
ELISA Test
0
5
10
15
50
100
105
110
115
120
125
dpi

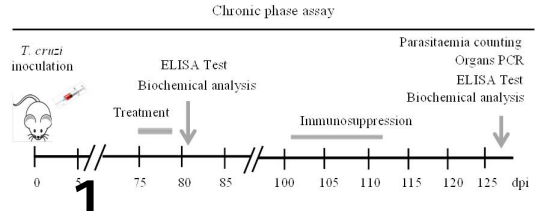
Chronic phase assay
T. cruzi inoculation
ELISA Test
Biochemical analysis
Treatment
Immunosuppression
Parasitaemia counting
Organs PCR
ELISA Test
Biochemical analysis
0
5
75
80
85
100
105
110
115
120
125
dpi

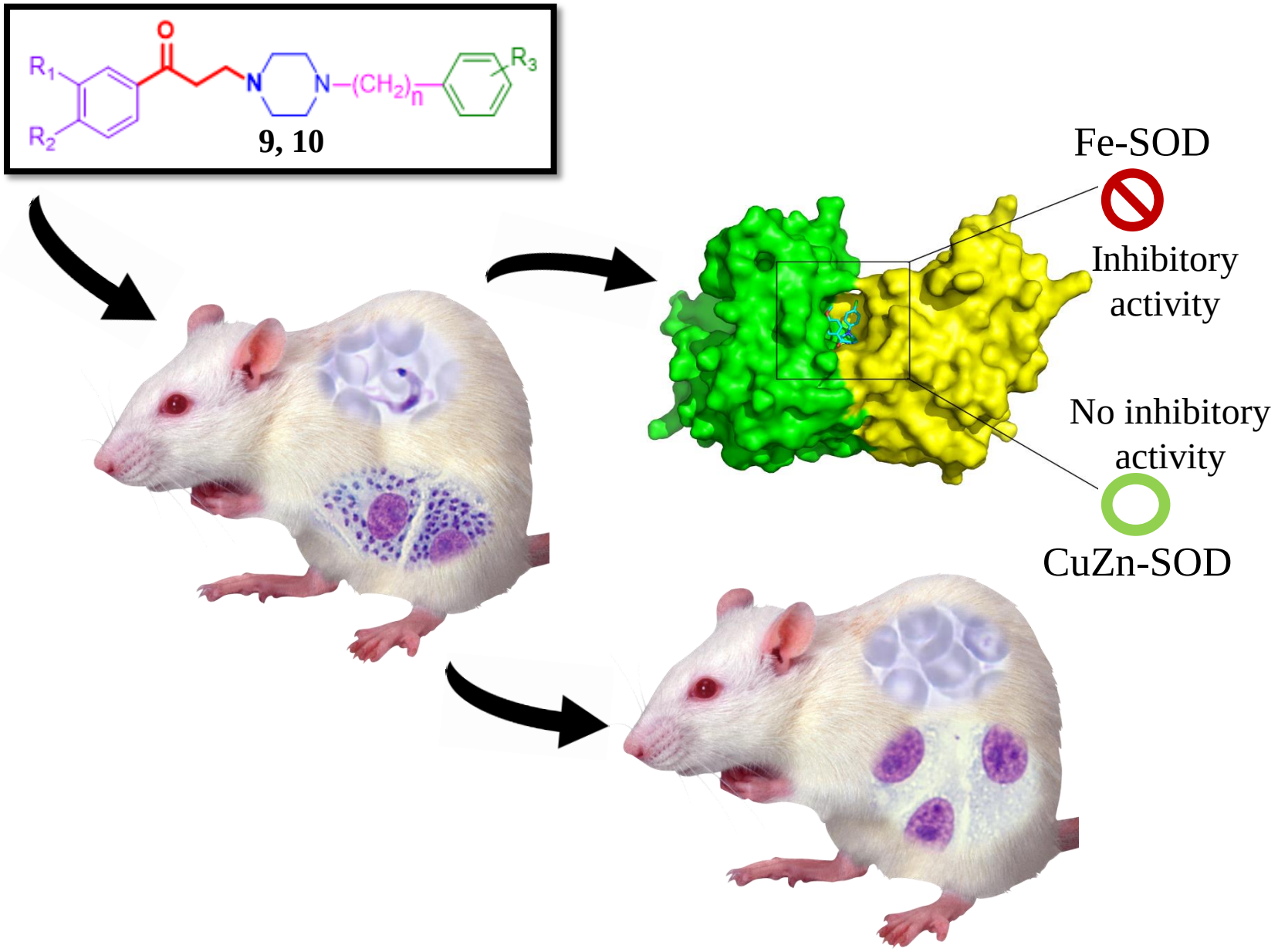
R1
R2
O
N
N
(CH2)n
R3
9, 10
Fe-SOD
Inhibitory activity
No inhibitory activity
CuZn-SOD